Estimation of Forging Die Wear and Cost

THESIS

Presented in Partial Fulfillment of the Requirements for the Degree Master of Science in the Graduate School of The Ohio State University

By

Adam R. Groseclose, B.S.

Graduate Program in Mechanical Engineering

The Ohio State University

2010

Master's Examination Committee:

Taylan Altan, Advisor

Gary Kinzel

Abstract

The estimation of forging die wear and cost are both important issues. Die wear accounts for a large portion (almost 70%) of die failures. This leads to increased costs to replace the die, through downtime and the cost of the die itself. Through finite element method (FEM), forging processes can be simulated and the die wear can be predicted. This allows for optimization of the forging process and increase in die life, as well as reduction in die try-out time and a proactive replacement of dies, which helps reduce scrap and downtime. Through two case studies of elevated temperature extrusion, it is shown that wear and plastic deformation prediction is possible. With these predictions, the extrusion processes can be improved for better die life and part quality in the future.

Accurate die cost estimation helps with early stage quoting processes. If a forger or purchaser is able to get an idea of the die costs, then it makes the whole procedure a little less of a guess. However, accurate quotes require a large amount of information. Thus, if it is possible to relate final part geometry to die cost, then a good estimate can be achieved almost immediately. The procedure to estimate cost has been outlined and the initial steps have been started.

Dedication

This document is dedicated to my family.

Acknowledgments

I would like to thank the sponsors of the following research: Hirschvogel Inc., Eaton Corp., Weber Metals Inc., and the Advanced Technology Institute (ATI), as well as all of the personnel of those companies which assisted me.

The assistance and opportunities provided by my advisor Dr. Taylan Altan were the key to my success. The support of Dr. Gary Kinzel and Dr. Jerald Brevick, along with other professors at The Ohio State University, was also very important in my academic and professional development. I therefore would like to thank them all for their time and efforts.

I also thank my fellow coworkers and friends of the Engineering Research Center for Net Shape Manufacturing (ERC/NSM). Yurdaer Demiralp, Nimet Kardes, Amin Al-Nasser, Jose Luis Gonzalez-Mendez, Ambikapathy Naganathan, Changhyok Choi, Mayur Deshpande, Partchapol (Jay) Sartkulvanich, Mary Hartzler, and Linda Anastasi, as well as many others, all helped me more than they can possibly imagine.

Lastly, I would like to thank my family for years of support and encouragement for which I could never repay. They are the foundation to which my education is built on and will continue to push me to bigger and better things.

Vita

December 30, 1985 ....Born, Norwalk, Ohio

June 2008 ....B.S. Mechanical Engineering, The Ohio State University, Columbus, OH

June 2008-June 2010......................................Graduate Research Associate, Engineering Research Center for Net Shape Manufacturing, The Ohio State University, Columbus, OH

Publications

“Evaluating Lubricant Performance for Stamping- Part I”, Stamping Journal, March 2009

“Evaluating Lubricant Performance for Stamping- Part II”, Stamping Journal, April 2009

“New Applications for Servo-Driven Presses- Part I: Stamping of Automotive Components”, Stamping Journal, June 2009

“New Applications for Servo-Driven Presses- Part II: New Technologies and Advancements”, Stamping Journal, July 2009

Fields of Study

Major Field: Mechanical Engineering

Table of Contents

List of Tables

List of Figures

Chapter 1: Introduction

Forging is an important process used in manufacturing; forged products exhibit excellent mechanical properties with a small amount or no material being wasted.

Cost of forging tooling has proved to be one of the most important factors in the overall process cost. Die costs range from 10% to 15% of the whole process cost. This includes cost of die material, machining the dies and subsequent heat treatment, when this is applied. Set up times can range anywhere from under 10 minutes to over 4 hours, resulting in additional direct wages in material handling, tool rework and other overhead costs. [Groseclose et. al., 2008]

In hot forging, the metal undergoes plastic deformation above its recrystallization temperature. Hot forging processes subject the dies to severe thermal and mechanical fatigue due to high pressure and heat transfer between the dies and the workpiece. High cyclic surface temperatures result in thermal softening of the surface layers of the dies, subsequently increasing die wear and susceptibility to heat checking. [Deshpande et. al., 2009]

In comparison to hot forging, warm forging offers advantages due to reduced energy costs of heating the workpiece to between 600°C and 950°C. Warm forgings also benefit from no scale formation, tighter tolerances and less subsequent machining. Warm forging also requires lower forming loads when compared to cold forging. [Groseclose et. al., 2008]

Forward extrusion processes are characterized by high sliding velocities and temperature generation. Very high normal pressures occur at die corner radii where a large reduction in area of the workpiece takes place. The primary failure mode in this process is generally abrasive wear. The dies must be removed from service and scrapped once the workpiece either a) is out of dimensional tolerance, b) exhibits poor surface finish, or c) sticks to the dies or transfer mechanisms. [Groseclose et. al., 2008]

Finite element analysis (FEA) has become a highly useful tool for forging companies that are in search of designing and developing new forging processes with little or no trial and error and significantly decrease lead time. One of the most important applications of FEA in the forging studies is the estimation of die wear, the FEA based prediction of die wear (fatigue fracture as well) has the following specific advantages: [Groseclose et al., 2008]

- Die changes can be scheduled based on the die life estimation, thus the time invested on re-setting a machine can be reduced.
- Forging parameters such as press speed, die materials, workpiece material and die temperatures can be optimized to increase die life.
- The effects of die geometry changes on die wear can be rapidly investigated.

Many input variables affect the reliability of the FEA in the study of die wear, including material properties of the workpiece, die geometry, die-workpiece interface, i.e. friction, lubrication, and heat transfer, and the characteristics of the forging equipment. Through computer aided engineering (CAE) and FEA, forgers are now able to produce parts with tighter tolerances and better surface finishes as well as maximize material utilization. [Groseclose et al., 2008]

Chapter 2: Background

Die Failure

Die failures for both warm and hot forging are very similar. Several factors impact the underlying physical phenomena behind die failure on forging processes: pressures, sliding velocities, hot hardness and a variety of physical and mechanical properties. From a process perspective, there are other several variables that impact die wear and tool failure. These include forging temperature, cycle times, and use of protective atmosphere during billet heating. [Shirgaokar, 2008]

Some authors have classified die failure mechanisms as follows [Shirgaokar, 2008]:

- Abrasive wear: Abrasive wear is the removal of material of the die surface caused by the sliding of a rough, hard surface against a softer material. In hot and warm forging abrasive wear is compounded by the presence of hard particles in the interface or variations inherent to the billet. In other words, abrasive wear can be defined as a die failure phenomenon where the die loses its original geometry over a period of time due to a constant abrasive action of particles across the die surface under high pressures during forging.
- Thermal fatigue: Thermal fatigue is defined as the crack appearance due to the repetitive changes of temperature; specifically the reason is the temperature difference between the die surfaces and its interior. Any temperature differences

between the surface and the interior results in stress and strain differential due to thermal expansion; when the resulting stress exceeds the hot strength of the material, yielding of surface layers is shown. Extended cycling will result in crack initiation and subsequent growth of thermal cracks.

- Plastic deformation: This mode of failure occurs at regions of the die that are subjected to extreme pressure and temperatures as well as long contact times. Mechanically speaking the local stresses result on die stresses that exceed the local hot yield strength of the die material. Typical areas of the die that tend to show this mode of failure are sharp corners of the dies and thin protuberances that trap a lot of heat during the forge.

While it is common to have more than one type of failure mechanism occurring in a single die, wear has been found to be the dominant reason for failure in forging, accounting for up to 70% of tool failures in production. [Shirgaokar, 2008]

Modeling Strategy

There are many models developed to estimate wear and most of those are based on Archard's wear model. The model used in this study is from Behrens' model, which is a modification of Archard's equation.

Behrens' model for die wear, given in Equation 1, computes wear depth at each forging cycle. The general formula sums from the first forging until a certain life cycle of the die (n). σ_N stands for the contact normal pressure, v_{rel} refers to the relative velocity between workpiece and tool, and Δt represents one time increment (inc). In this case hardness (H) depends on temperature and process duration *t*, *k* is a wear coefficient that needs to be calibrated in order to calculate wear quantitatively [Behrens, 2008].

It is important to note that particularly for this proposed model the workpiece temperatures reach up to 1300°C, which will lead the forging die to a tempering range, under this statement hardness will be calculated by: first estimating a tempering parameter (dependant on time and temperature), and then such parameter will be included in a quadratic function of hardness for the die material, H(θ,t).

$$w = k \sum_{inc=1}^{n} \left[\left[\frac{\sigma_N}{H(\theta,t)} \right] v_{rel} \cdot \Delta t \right] inc \qquad \text{Equation 1}$$

In this study, the total wear depth is expressed as the integral function, Equation 2, with respect to time (t) during a single forging cycle.

$$W_n = \sum_{j=1}^{n} K \int \left(\frac{P}{H_{hot}(d_j, M_j, T)} \right)^a V dt \qquad \text{Equation 2}$$

The wear equation used to predict the wear depth is given by Equation 2, where $\boldsymbol{W_n}$ is the wear depth after the $\boldsymbol{n}^{th}$ forging cycle, $\boldsymbol{K}$ is the abrasive wear coefficient, $\boldsymbol{P}$ is the normal pressure (MPa) on the contact surface, $\boldsymbol{H_{hot}}$ is hot hardness (Vickers hardness, MPa), $\boldsymbol{V}$ is the sliding velocity (mm/sec) at the contact surface, $\boldsymbol{a}$ is an experimental constant, $\boldsymbol{M_j}$ is the tempering parameter, $\boldsymbol{d_j}$ is distance from surface(mm) at the $\boldsymbol{j}^{th}$ forging cycle, and $\boldsymbol{T}$ is the temperature (°C).

Initial hardness (H_i)

Initial hardness can be controlled by heat treatment and surface treatment.

- Initial hardness on the base metal depends on heat treatment, quenching temperature, tempering temperature, and time.
- Initial hardness on the surface metal depends on surface treatment such as nitriding temperature and time.

$$H_i(d) = C_0 - C_1(1 - \exp(-C_3 \cdot d)) \qquad \text{Equation 3}$$

$$C_2 = -\frac{\ln\left(1 + (H_{90\%} - C_0)/C_1\right)}{d_{nitride\ layer}} \approx \frac{2.3}{d_{nitride\ layer}} \qquad \text{Equation 4}$$

In order to consider the change in the initial hardness due to nitride layer, a function with respect to distance from surface (***d***) is defined given by Equation 3. It was assumed that the hardness of the dies decreases exponentially from the initial surface hardness equal to that of the nitride layer to the hardness of the base metal, where $\boldsymbol{H_i}$ is initial hardness (HV, MPa) at the distance from surface (***d***), $\boldsymbol{C_0}$ is the maximum hardness on the surface, and $\boldsymbol{C_1}$ is the range of hardness between hardness on the surface and hardness of the base metal, and $\boldsymbol{C_2}$ is the function of distance, Equation 4, where the hardness decreases to 90% between hardness on the surface and hardness of base metal, and $\boldsymbol{d_{nitride\ layer}}$ is the total depth of nitride layer (mm).

*Room temperature hardness (**H_{room}**)*

Initial hardness is changed due to high temperature and holding time

$$H_{room} = H_i \cdot F_{soft}(M) \qquad \text{Equation 5}$$

In order to find the room temperature hardness with change in tempering parameter (***M***), room temperature hardness (***H_{room}***) is defined as in Equation 5, where ***H_i*** is initial hardness (HV, MPa) and ***F_{soft}*** is thermal softening factor at the tempering parameter (***M***). Thermal softening factor can be obtained from the tempering curve, tempering temperature versus room temperature hardness from the literature. [Nachi-Fujikoshi, 2008]

*Hot hardness (**H_{hot}**)*

Hardness of the dies decreases with increase in temperature

$$H_{hot} = H_{room} \cdot F_{hot}(T) \qquad \text{Equation 6}$$

In order to find hot hardness (***H_{hot}***), a function with respect to instantaneous temperature (***T***) is defined in Equation 6, where ***F_{hot}*** is hot strength factor at the instant temperature (***T***), and ***H_{room}*** is room temperature hardness (HV, MPa).

Hot strength factor can be obtained from the hot hardness curve or hot strength curve from the literature [Nachi-Fujikoshi, 2008].

$$H_{hot}(d, M, T) = H_i(d) \cdot F_{soft}(M) \cdot F_{hot}(T) \qquad \text{Equation 7}$$

*Tempering parameter (**M**)*

Tempering parameter (***M***) is given by Equation 8. As the temperatures of the die surface change during forging, the equivalent temperature ($\boldsymbol{T_{eq}}$) is used as the maximum temperature during cycle duration. [Behrens, 2008] Where, $\boldsymbol{h_{eq}}$ is equivalent tempering time (hr) and ***h*** is total forging cycle time (hr).

$$M = T_{eq}(20 + \log_{10}(h_{eq} + h)) \qquad \text{Equation 8}$$

$$h_{eq} = \sum_i 10^{\left(\frac{T_i}{T_{eq}}(20+\log_{10} h_i)-20\right)} \qquad \text{Equation 9}$$

- Equivalent tempering time equation ($\boldsymbol{h_{eq}}$) is given by Equation 9.

Where, $\boldsymbol{T_i}$ is tempering temperature (K) at the $\boldsymbol{i}^{\text{th}}$, $\boldsymbol{h_i}$ is tempering holding time (hr) at the $\boldsymbol{i}^{\text{th}}$.

To determine *K* and *a* (wear equation constants), the experimental data must be compared with FEM results. Experimental dies are measured with CMM to obtain the final “worn” profile. The microhardness of the dies is also taken before and after the die trials (to give the initial and final hardness).

Using FEM, the process parameters (normal pressure, relative velocity, and time) are determined for the wear equation. The FEM results combined with the hardness and CMM data allow for the experimental constants, *K* and *a*, to be calculated.

There is one issue with the above methodology. The CMM data (the “worn” profile) is assumed to only contain abrasive die wear. However, in practice there is also plastic deformation of the dies observed. Thus, the CMM data contains the information of the abrasive wear and the plastic deformation.

To get the true wear profile, the plastic deformation is estimated through FE simulation and this new deformed geometry is compared to the CMM data. The difference between the CMM data and the deformed die geometry is the abrasive wear.

To obtain the plastically deformed die geometry, a series of FE simulations must be performed.

- Multiple simulations with rigid tooling to determine the steady state temperature distribution in the dies
- The assembled tooling (now elastic) is disassembled and allowed to thermally expand
- The elastic and thermally expanded tooling is then reassembled to apply compressive stresses
- The assembled extrusion die (now elasto-plastic) and the other tooling (elastic) are used to form the workpiece (plastic) in one simulation
- The tooling is disassembled and the extrusion die (elasto-plastic) is allowed to cool to room temperature
- The cooled extrusion die retains the plastic deformation from the forming simulation

To simulate the plastic deformation of the extrusion die, it is necessary to determine the flow stress of the die material (illustrated in Figure 1). The traditional flow stress equation is function with respect to effective strain **(**), effective strain rate ( ), and temperature (***T***).

In order to consider die softening due to forging temperature and time, flow stress function ( ) with respect to tempering parameter (***M***).

$$\begin{aligned}\bar{\sigma}(\bar{\varepsilon},\dot{\bar{\varepsilon}},T,M) &= \bar{\sigma}(\bar{\varepsilon},\dot{\bar{\varepsilon}},T)\times\frac{H_{room}(M)}{H_0} \\ &= \bar{\sigma}(\bar{\varepsilon},\dot{\bar{\varepsilon}},T)\times\frac{H_i}{H_0}\times F_{soft}(M)\end{aligned} \qquad \text{Equation 10}$$

The flow stress equation used to predict plastic deformation is given by Equation 10, where H_{room} is room temperature hardness (HV, MPa) of the dies, H_i is initial hardness (HV, MPa) of the dies, H_0 is initial hardness(HV, MPa) of the material data of the traditional flow stress function.

Now that the deformed die geometry is known, the abrasive wear profile is known. Since the wear profile is known, the wear model can be applied and the equation constants can be calculated. Using the constants, the wear of future dies can be predicted.

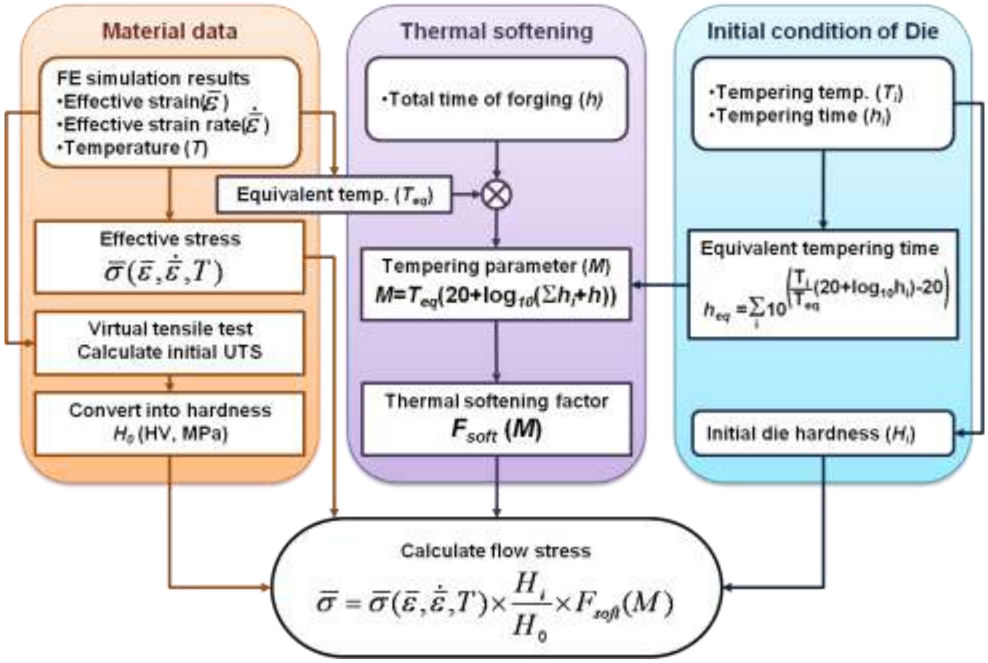

Figure 1: Flow Chart to Determine the Die Material Flow Stress

Chapter 3: Research Focus and Objectives

Die Wear

Warm and hot forging processes subject the dies to extreme temperatures due to heat transfer between the dies and workpiece. The thermal cycling of the die surface causes softening in the surface layers of the die, which decreases wear resistance. The dies also experience mechanical fatigue because of high pressures at the die-workpiece interface. In forward extrusions, a large reduction in cross section of the workpiece substantially increases the velocity at which the material is flowing. This velocity, in conjunction with the pressure at which the material flows, affects the wear rate of the material. [Groseclose et. al., 2008]

Two case studies are presented in the following research. The first is the warm extrusion of steel pinion shafts for automotive applications. The second is the hot forging of engine valves (which includes both an extrusion and a coining process), also for automotive applications. Both of these studies are on axisymmetric parts and FEA is implemented to obtain process variables.

The following focus areas were selected for this research project in cooperation with the forging industry and Hirschvogel Incorporated (Case Study 1- Pinion Shaft) and the Department of Energy and Eaton Corporation (Case Study 2- Exhaust Valves):

Determination of process conditions (including part temperatures, die temperatures, die stresses, forming pressures and velocities) of the extrusion process (Case 1 and 2) and coining process (Case 2) during start up and steady state conditions.

Prediction and estimation of die wear using existing wear models and FEM solutions.

The results of these studies are obtained through a combination of computer simulations and validation from production trials.

Die Cost

Die costs for low quantity runs are very important. To estimate these costs is difficult and usually based on knowledge and experience, rather than empirical formulas. Therefore, a project in cooperation with the DLA, ATI, and University of Toledo was conducted to determine the cost of forging dies. The following objectives were determined for the project:

- Review of cost models in literature
- Determination of current practice of cost estimation and die production in industry
- Validation of cost models
- Development and validation of cost model based on obtained data from Weber Metals

The final result is to have a cost model which can give a preliminary estimation (within a reasonable error of the actual die cost) of die cost with a minimal amount of initial information. Therefore, it is to use the geometric and physical properties of the forging to estimate the die cost. Once the model is developed, it is to be implemented in a computer code that is easily accessible, such as Microsoft Excel.

Chapter 4: Finite Element Analysis

Case Study 1- Steel Pinion

Steel pinions are warm forged, which has benefits over cold and hot forging. Warm forging benefits include less heating, tighter tolerances, no scale formation, and less subsequent machining over hot forging. Warm forging also requires lower forming force than cold forging. [Groseclose et. al., 2008] The studied process (in cooperation with the Forging Industry Education and Research Foundation and Hirschvogel, Inc.) is a three step forming procedure. The forming is as follows; 1) forward extrusion, 2) upsetting, and 3) coining. However, this particular study focused on the first forward extrusion stage.

The pinion is formed in an automated system that includes a pre-lubrication station, induction heater, and a mechanical press (which contains all three forming stages), as well as an automated part transfer system and die lubrication. The press also has a data acquisition system which records the process cycle time and forging load.

The studied extrusion die is made of tool steel (various materials were tested, but DURO-F1 is presented in this thesis) and involves three reductions (Figure 2). The billet material is a round billet (approximately 70 mm diameter and 200 mm length) made of AISI 8620 steel and heated to 960-980˚C.

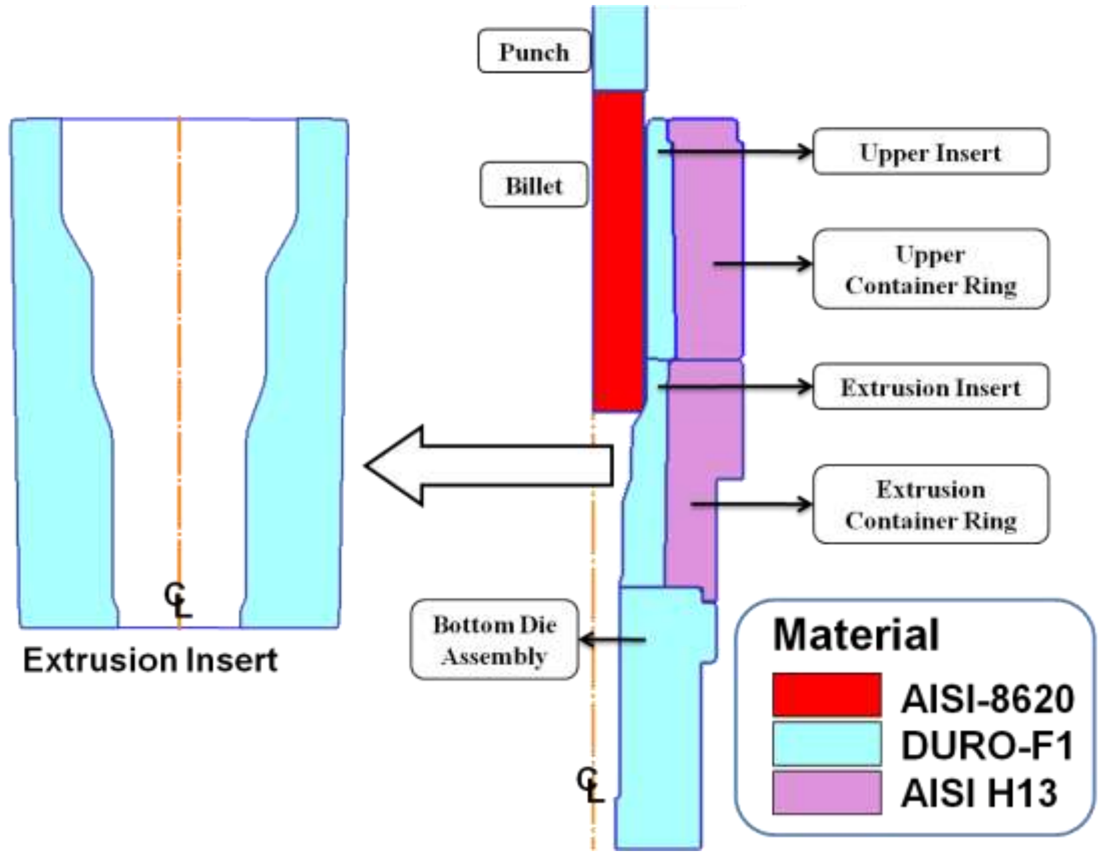

Figure 2: Schematic of Extrusion Tooling and Extrusion Insert Detail

Calculation of Steady State Die Temperatures

To calculate the steady state die temperatures, the tooling is assembled in DEFORM-2D using rigid dies and is initially at room temperature (20˚C). The billet forming is then simulated, including all the process times and heat transfers. The incremental die temperature increase is captured through DEFORM Multi-Operation, which is used to simulate 100 consecutive forging cycles. After 50 cycles, the temperatures in the die are assumed to be “steady state”. The simulation inputs for one cycle are shown in Table 1.

Variable	Value	Source
Billet Initial Temp. [˚C]	970	Hirschvogel
Tooling Initial Temp. [˚C]	20	Hirschvogel
Press Speed [SPM]	63	Hirschvogel
Process Times [sec]	Varies	Hirschvogel
Heat Convection Coefficient (Air) [kW/m^2-K]	0.02	DEFORM
Heat Transfer Coefficient (during forging) [kW/m^2-K]	11	DEFORM
Heat Transfer Coefficient (during free-resting) [kW/m^2-K]	1	DEFORM
Heat Transfer Coefficient (during lubrication) [kW/m^2-K]	35	[Shirgaokar, 2008]
Shear Friction Coefficient	0.3	DEFORM
Billet Material Properties	-	DEFORM
Tooling Material Properties	-	DEFORM
Ambient Temp. [˚C]	20	[Shirgaokar, 2008]

Table 1: FEM Input

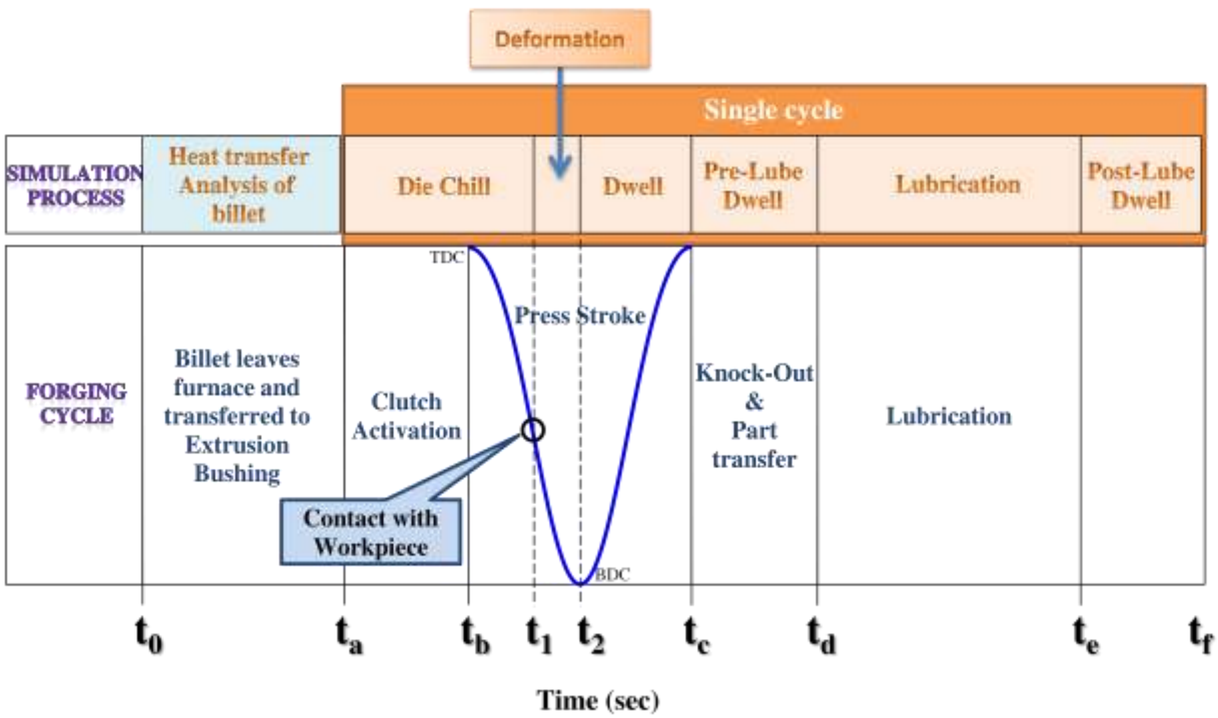

Figure 3: Description of a Forging Process on a Mechanical Press

The process timing (Figure 3) are as follows:

- Part location ($t_0 - t_a$): The billet is exposed to the environment from the time it exits the induction heater until it is finally placed in the extrusion die.
- Die chill time ($t_a - t_1$): Time from when the billet is placed on the die until the punch (top die) makes contact with the billet.
- Deformation time ($t_1 - t_2$): Determined to be 0.133 seconds from press kinematics.
- Knockout and part removal ($t_e - t_f$): Estimated to be a few seconds.
- Lube spray ($t_d - t_f$): The lubricant is sprayed into the upper and lower dies for a very short time, which is followed by a short dwell until the start of the next cycle.
- The total cycle time for forging in one station is ($t_f - t_a$).

All of these process steps were included into the FE simulations. The heated billet was allowed to cool in the ambient environment, until it is placed in the extrusion die. This produces temperature gradients in the billet (Figure 4). The billet cools further after being placed in the die until deformation starts. The die temperatures increase during deformation and the temperatures start to distribute during the part removal. Dies cool during the lubricant application and dwell before the next billet is received. This temperature variation can be seen in Figure 5, which shows the maximum temperature in the die with respect to the cycle time for the 1^{st}, 50^{th}, and 100^{th} cycles.

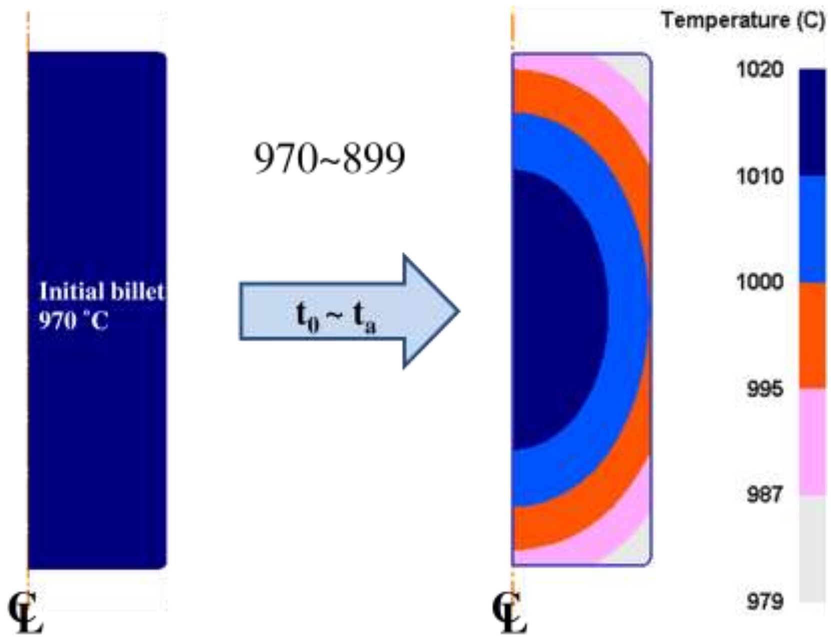

Figure 4: Billet Temperatures Before (left) and After (right) Cooling

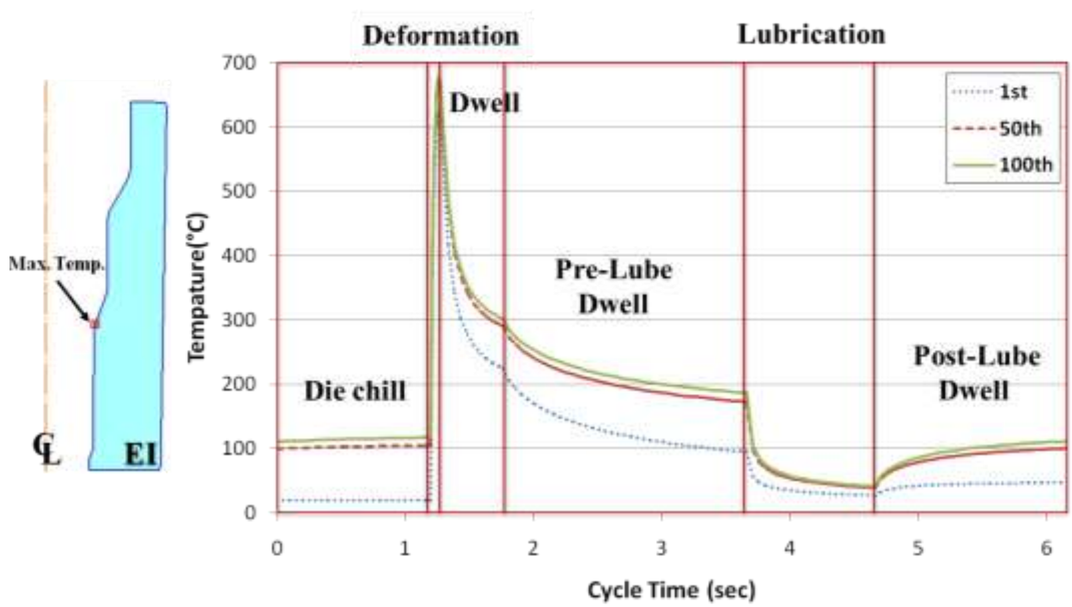

Figure 5: Temperature Variation at the Maximum Temperature during the 1st, 50th, and 100th Cycle

The die temperatures at the end of the cycle are higher than at the start. The next cycle is started with the temperature distributions from the previous cycle. This process was continued for 100 cycles and the steady state temperature distributions are shown in Figure 6. The die temperature variation (and increase to steady state) can be seen in Figure 7.

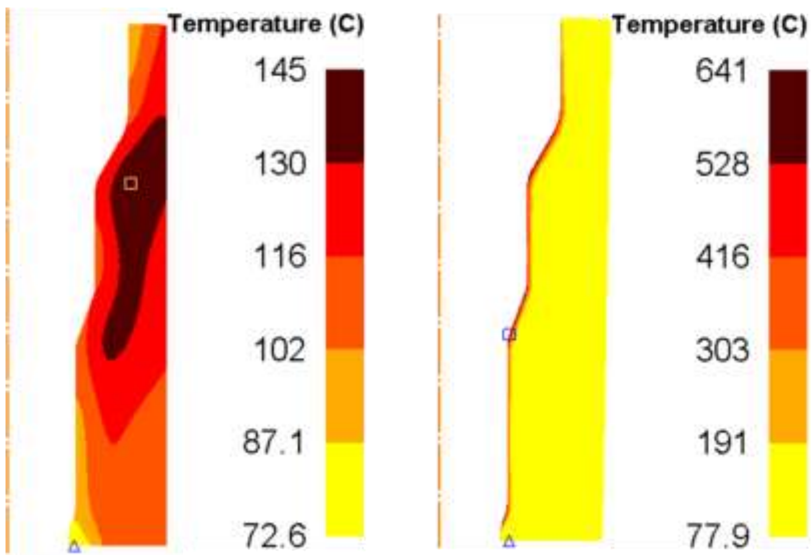

(a) At the start of cycle (b) After deformation

Figure 6: Steady State Temperature Distribution of the Extrusion Insert for the 100th Cycle

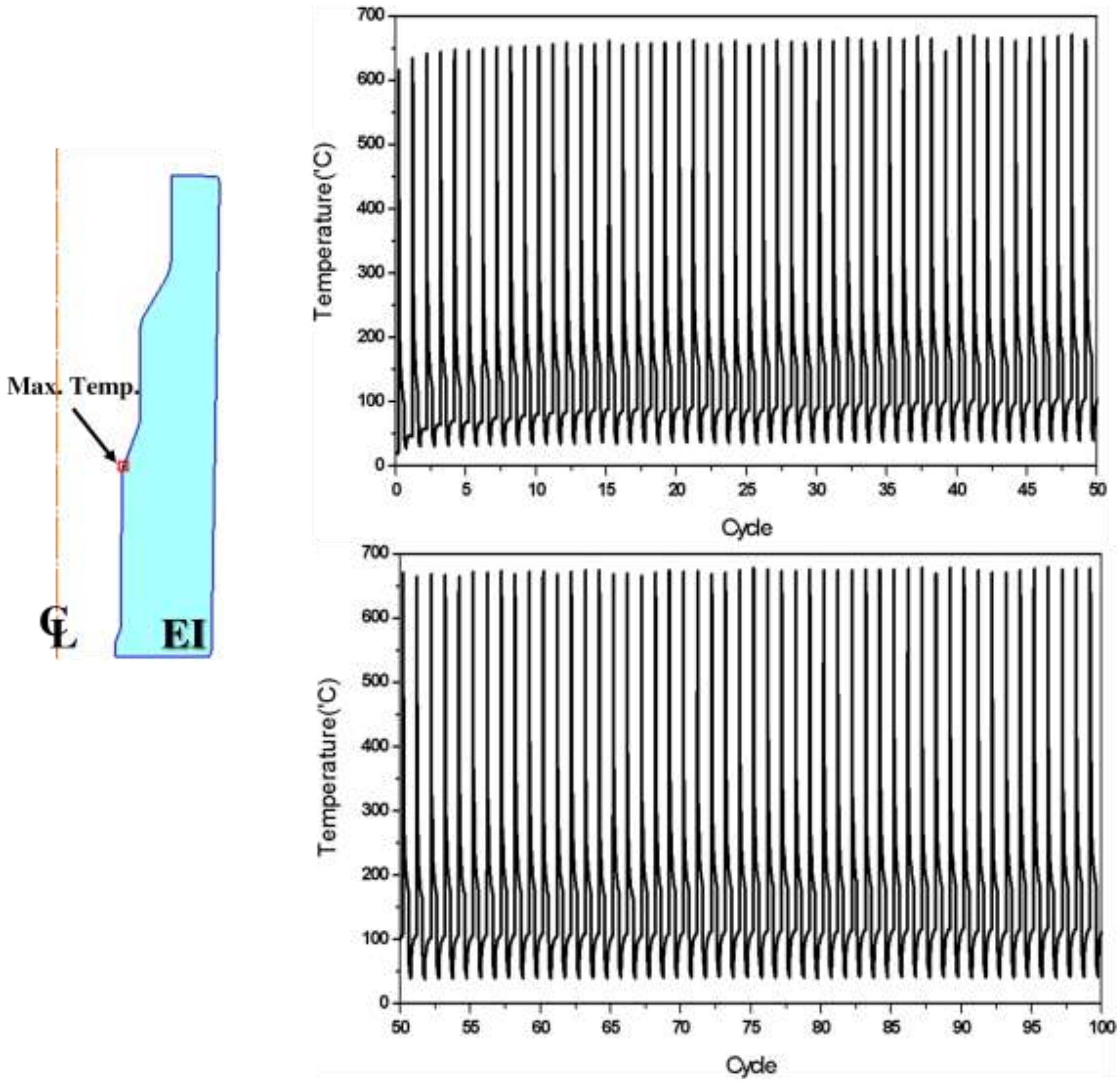

Figure 7: Maximum Temperature Variation for 100 Cycles

Prediction of Plastic Deformation of Die

After obtaining the steady state temperature distribution, the plastic deformation of the die can be predicted. The plastic deformation can be estimated through a series of FEA simulations and a flow stress model for the tool steel. The flow stress model (discussed in

Chapter 2) is based on the material data given by the manufacturer (Nachi-Fujikoshi). Along with the material data, micro-hardness measurements were taken of the initial die (prior to being used in production) and the flow stress for the given material at the given initial conditions was determined.

With the flow stress model and steady state temperatures, the FEA simulations are conducted. The simulations follow the previously discussed process (Chapter 2). Figure 8 shows a flow chart of the process.

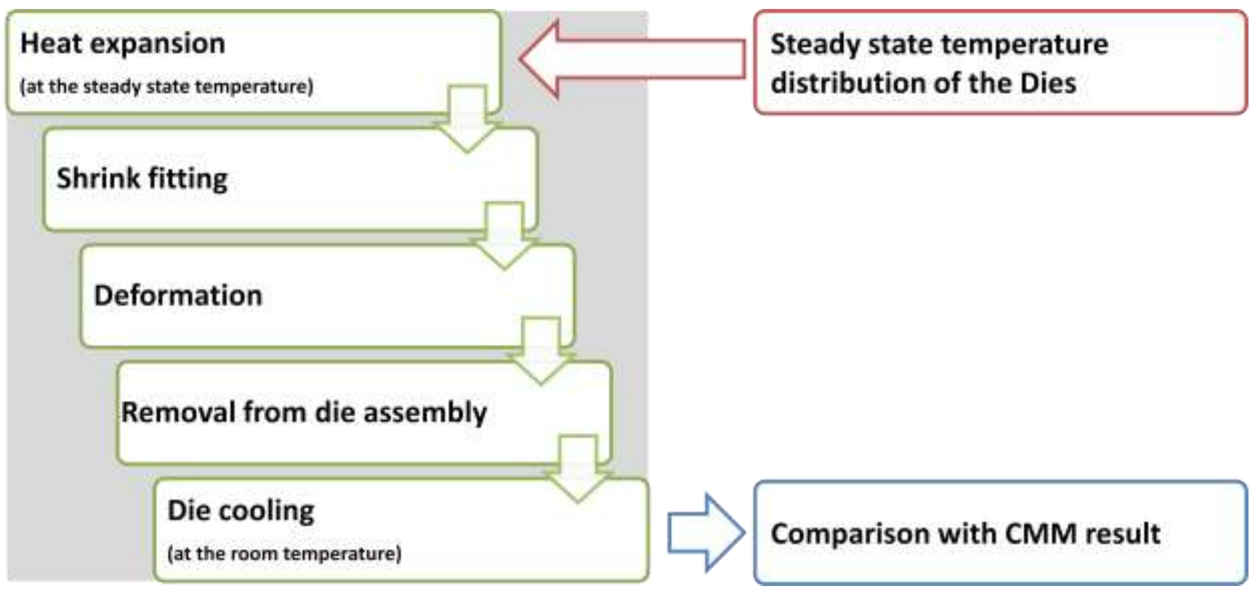

Figure 8: Flow Chart of FEA Prediction of Plastic Deformation of Extrusion Die

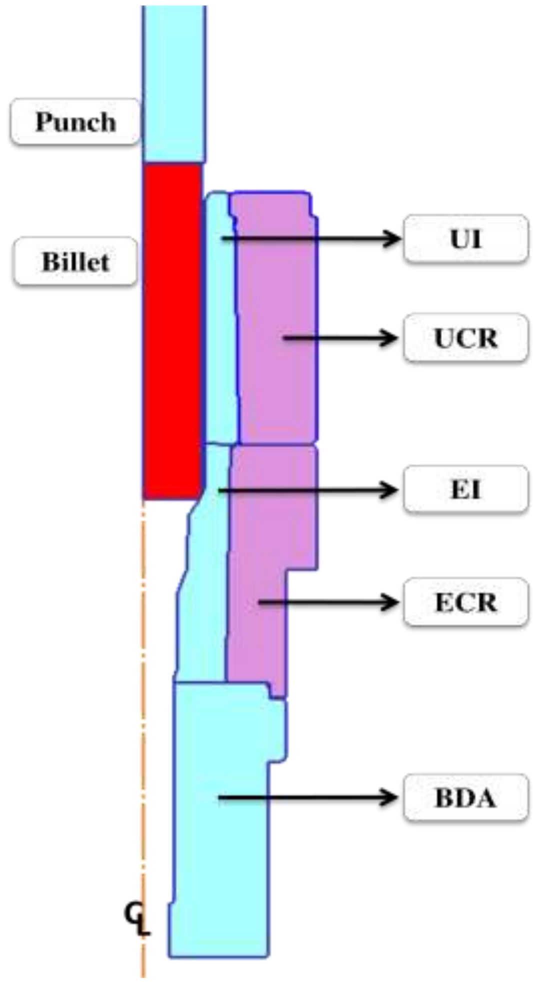

Figure 9: Schematic of Extrusion Tooling

FEA Simulations	**EI**	**UI, UCR, ECR**	**Punch, BDA**
Heat expansion	Elastic	Elastic	Rigid
Shrink fitting	Elastic	Elastic	Rigid
Deformation	Elasto plastic	Elastic	Rigid
Removal from die assembly	Elasto plastic	Elastic	Rigid
Die cooling	Elasto plastic	Elastic	Rigid

Table 2: Summary of FEA Simulations and Tooling Material Conditions

The results for the simulations are shown in Figure 10 for 1800 forging cycles. The elastic and plastic deformation (during the deformation process of extruding the pinion) of the die is shown by the dashed line and labeled ‘after deformation’. The plastic deformation after all loads have been removed (mechanical and thermal loads) is illustrated in the solid line, labeled ‘after die cooling’.

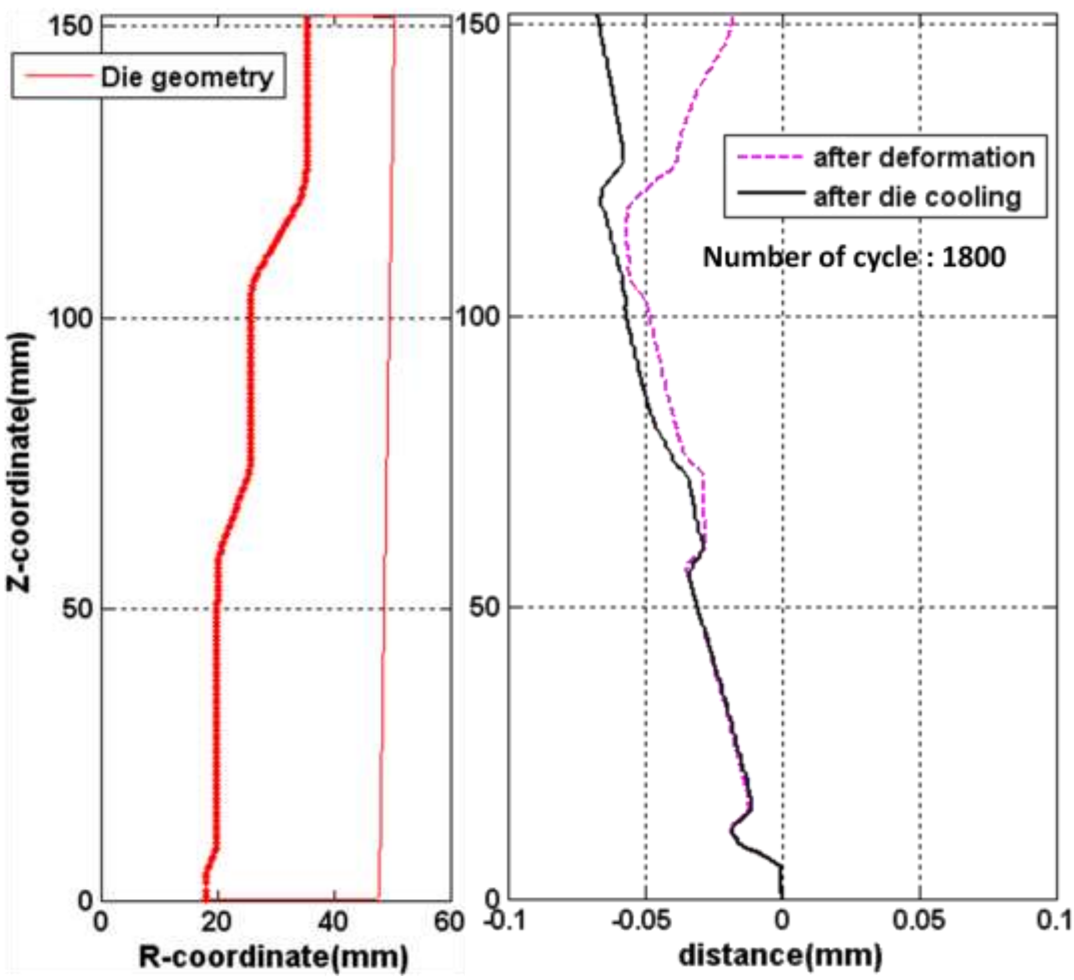

Figure 10: Initial Die Geometry (left) and Deformation of the Die (right), Elastic and Plastic Deformation including Thermal Deflections (dashed line) and the Plastic Deformation (solid line)

Prediction of Abrasive Die Wear

The die wear prediction is completed after the plastic deformation is estimated. Using the FEA simulation results from the die temperature and plastic deformation analyses, all the information to estimate wear is known. The plastic deformation analysis gives the die geometry to compare with the CMM data measurement. However, it also provides the other information needed to use the wear equation.

$$W_n = \sum_{j=1}^{n} K \int \left(\frac{P}{H_{hot}(d_j, M_j, T)} \right)^a V dt \qquad \text{Equation 11}$$

H_{hot} is the hot hardness of the die material and it is determined based on the material properties. The normal pressure, P, relative velocity, V, and time, dt, are all provided by the FEA simulations. For each node during the deformation process, there is a P and V value, and these are averaged over time, dt. The results are shown in Figure 11 for the average pressure and velocity with respect to the location on the die surface.

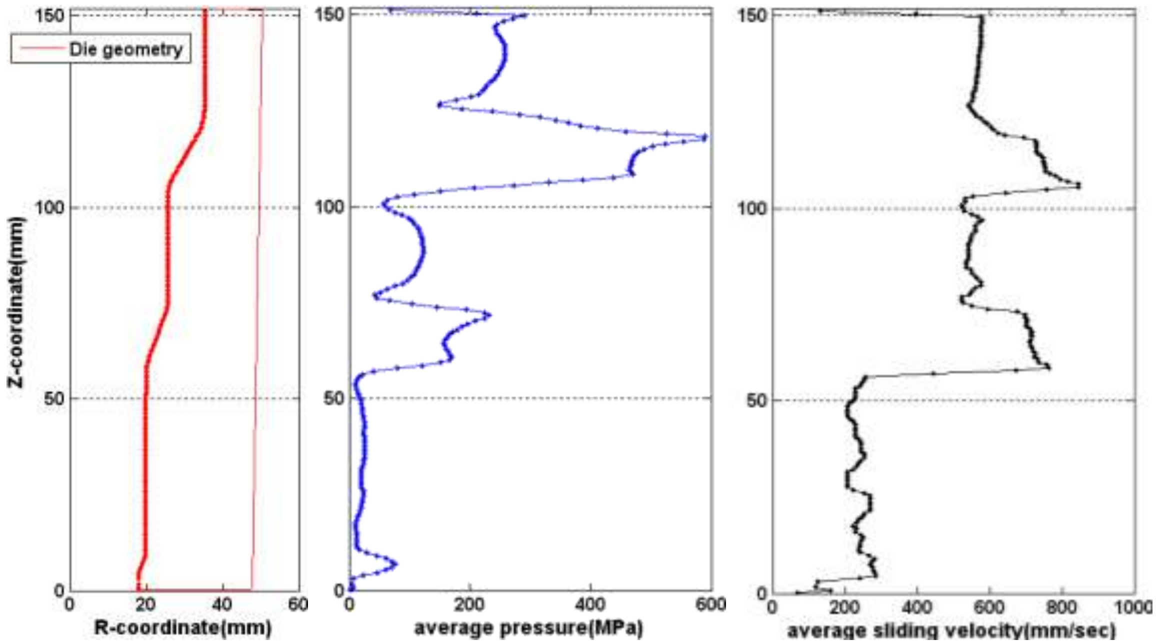

Figure 11: Average Pressure (middle) and Sliding Velocity (right) versus the Location on the Die Surface (left)

Case Study 2- Engine Exhaust Valve

In cooperation with a major company, a study to predict die wear in the hot forging of engine exhaust valves was conducted. These valves are formed in two steps: 1) an extrusion operation and 2) a coining operation. Both processes were simulated, but only the wear of the extrusion die was predicted.

The extrusion and coining occur on the same press in separate die sets. The press is a mechanical press operating in an intermittent mode, which is when the press runs at a speed of 60 to 90 strokes per minute and at the top dead center (TDC) the ram is stopped to allow for part transfer. This gives an effective production rate of about 15-30 parts per minute.

The valve forming process is automated and includes; induction heater, extrusion tooling and coining tooling on a mechanical press, as well as an automatic part transfer system and lubrication systems. The press is rigged with stress bars to allow for measurement of the total forming force on the press frame.

The extrusion die is made of AISI H-10 and is a single reduction extrusion with a radius. The schematic of the extrusion tooling is in Figure 12. The billet is round and made of stainless steel. The billet is heated to about 1000 to 1200˚C before being extruded.

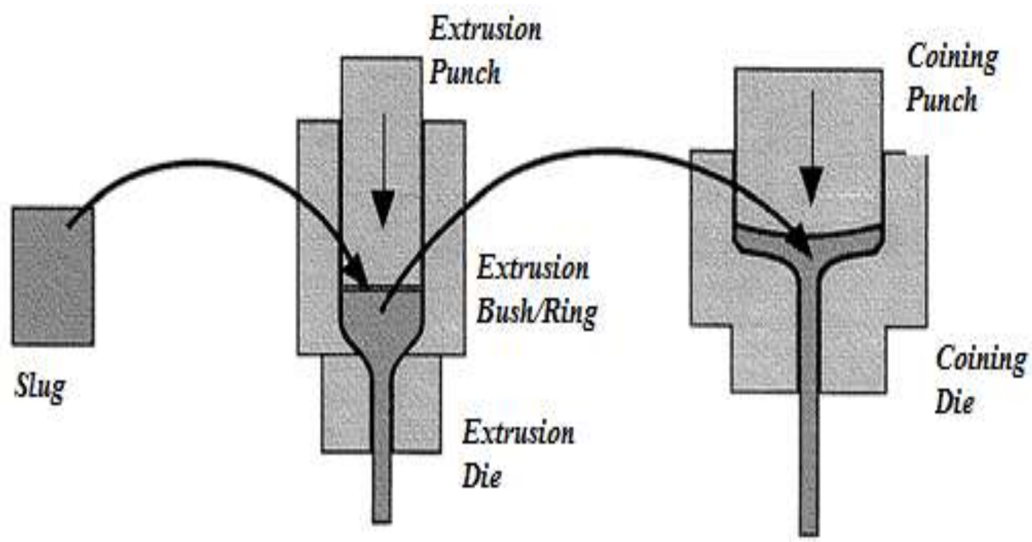

Figure 12: Schematic of Extrusion Tooling (middle) and Coining Tooling (right). [Deshpande et. al., 2009]

Calculation of Steady State Die Temperatures

The steady state temperatures are calculated similarly to Case Study 1. The tooling is assembled at room temperature with rigid dies in DEFORM-2D. Then 50 cycles were simulated with DEFORM Multi-Operation to obtain the steady state temperature distributions. The simulations for the extrusion and coining tooling were conducted separately, using the appropriate input data for deform.

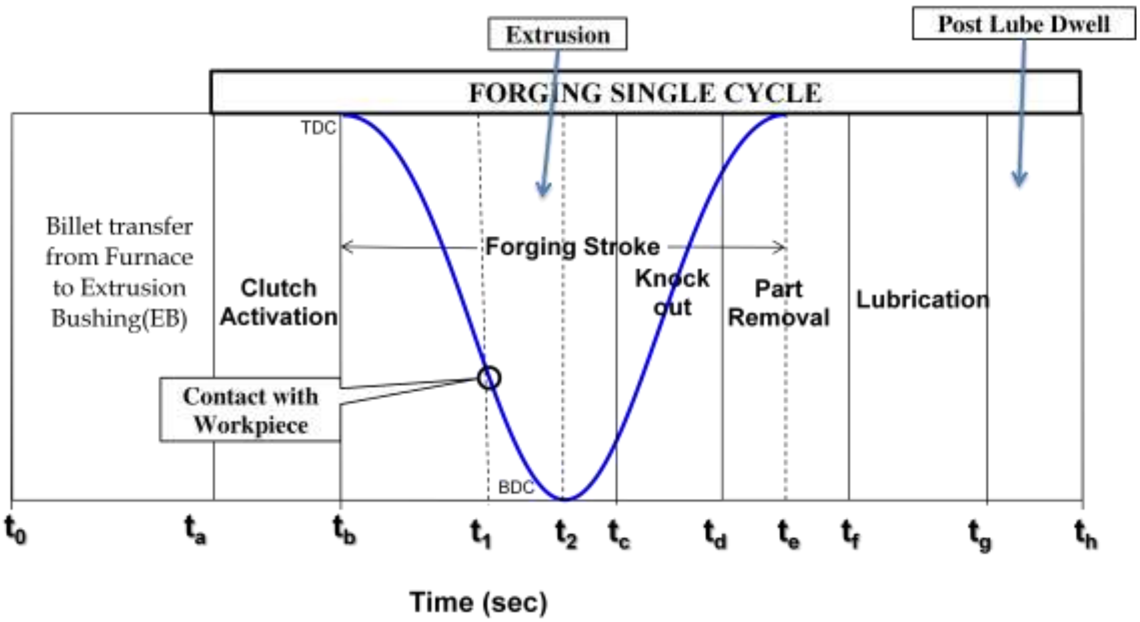

Figure 13: Valve Extrusion Process Sequence

The extrusion process sequence is illustrated in Figure 13 and consists of:

- Billet Transfer (t_a – t_0): The time for which the billet is exposed to the environment, i.e. from the time it exits the induction heater until it is placed inside the extrusion bushing.
- Clutch activation time (t_b – t_a): It is the time taken by the press driving mechanism to start the ram movement.

- Forging Stroke (t_e – t_b): It is the time taken by the press to move from the Top Dead Center (TDC) to Bottom Dead Center (BDC) and back to Top Dead Center.
- Extrusion/Deformation time (t_2 – t_1): It is the time from when the punch touches the billet until it reaches BDC. The deformation time is determined from press kinematics.
- Knockout (t_d – t_c): The knockout punch starts to move upwards to push the forged part out of the extrusion die.
- Part removal (t_f – t_d): The time required for the turret to transfer the extruded part from the extrusion die to the coining die.
- Lubrication (t_g – t_f): The time during which the lubricant is applied.
- Post Lubrication dwell (t_h – t_g): It is the time from when the lubricant application is stopped until the start of the next forging cycle.
- The total cycle time for extrusion is (t_h – t_a).

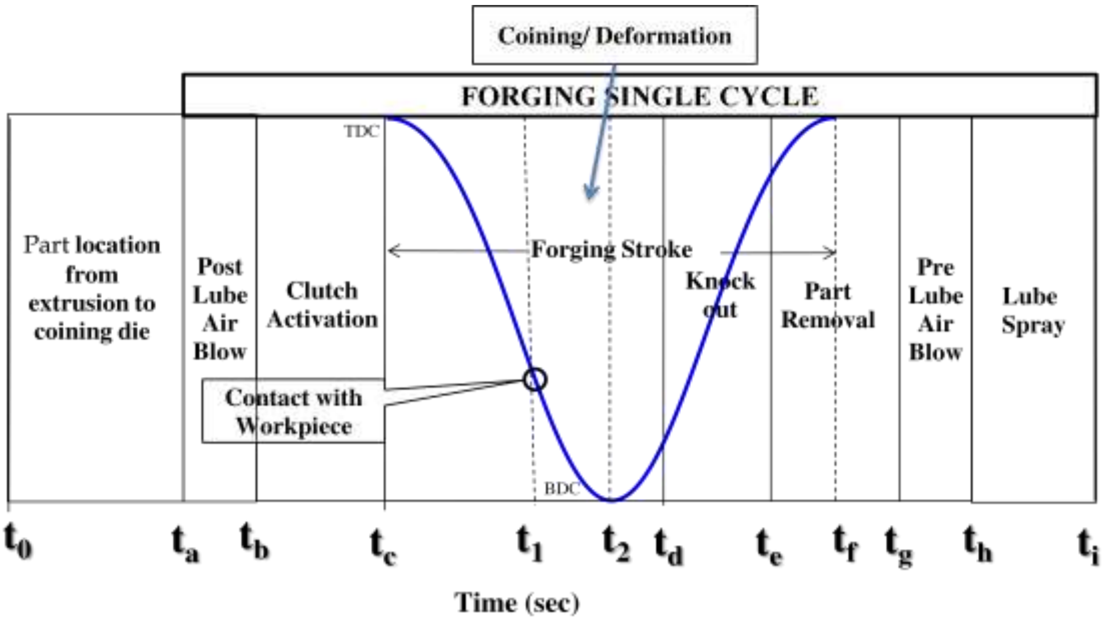

Figure 14: Coining Process Sequence

The process sequence for the coining operation (Figure 14) is similar to that for extrusion, although there are some differences in the lubrication. The coining process consists of:

- Part location from extrusion to coining die ($t_a - t_0$): The time for which the workpiece is exposed to environment.
- Post Lube Dwell ($t_b - t_a$): Time after lubrication is applied and prior to workpiece being placed in die.
- Clutch activation time ($t_c - t_b$): It is the time taken by the press driving mechanism to start the ram movement.

- Forging Stroke ($t_f - t_c$): It is the time taken by the press to move from the Top Dead Center (TDC) to Bottom Dead Center (BDC) and back to TDC.
- Coining/Deformation time ($t_2 - t_1$): It is time from when the punch touches the extruded preform until it reaches the BDC. The deformation time is determined from press kinematics.
- Knockout ($t_e - t_d$): The knockout punch starts to move upwards to push the forged part out of the coining die.
- Part removal ($t_g - t_e$): The time required for the transfer of the forged valve out of the coining die.
- Pre Lube Dwell ($t_h - t_g$): Time before lubricant is applied.
- Lube Application ($t_i - t_h$): The lubricant is applied onto the coining die and punch.
- The total cycle time for coining is ($t_i - t_a$). (which is same for Extrusion)

All of the process steps were included into the FE simulations for both the extrusion and coining die. The billet cools during transfer from the heater to the first die (Figure 15). The die temperatures increase during deformation and the temperatures start to distribute during the part removal. For coining, the preform (from extrusion) cools while being transferred to the coining die and the temperatures are shown in Figure 16. Dies cool during the lubricant application and dwell before the next billet is received. The temperature variation can be seen in Figure 17 (for extrusion) and Figure 18 (for coining), which shows the maximum temperature in the die with respect to the cycle time for the 1st, 25th, and 50th cycles (extrusion) and for the 1st and 50th (coining).

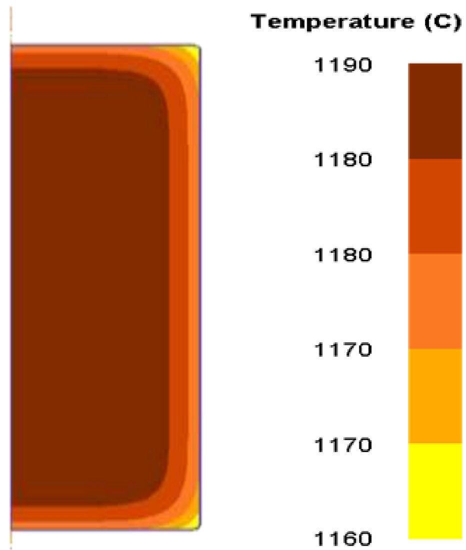

Figure 15: Billet Temperatures after Environment Exposure [Deshpande et. al., 2009]

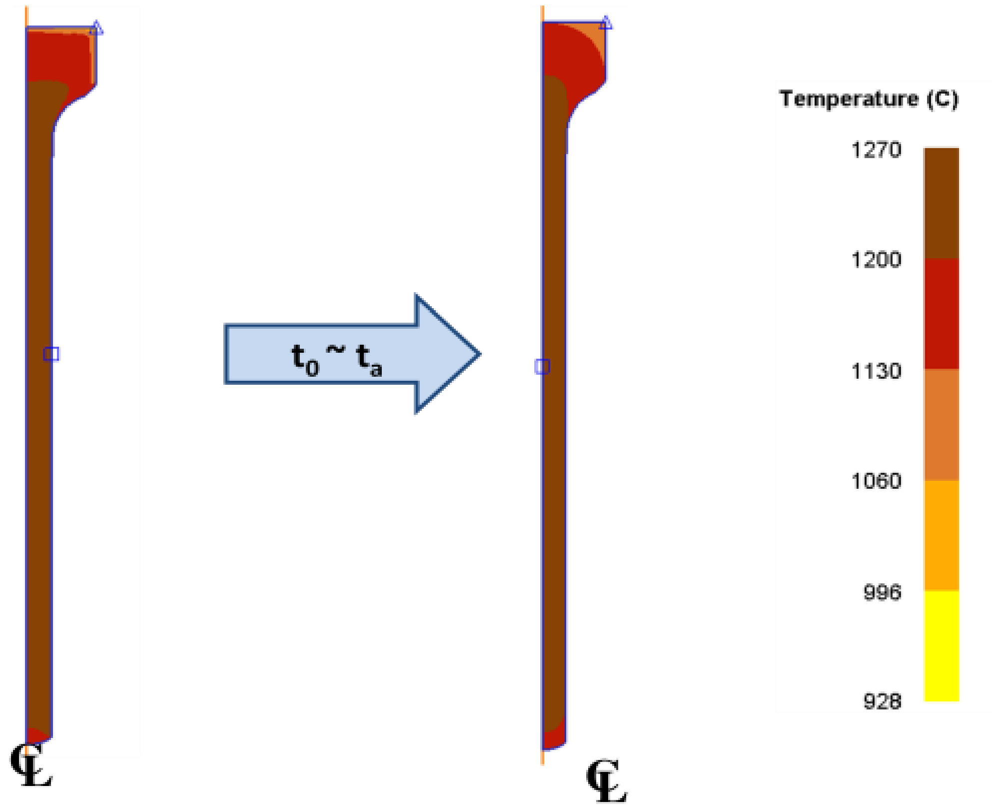

Figure 16: Change in Temperature Distribution in Preform as it is Transferred from Extrusion to Coining Tooling [Deshpande et. al., 2009]

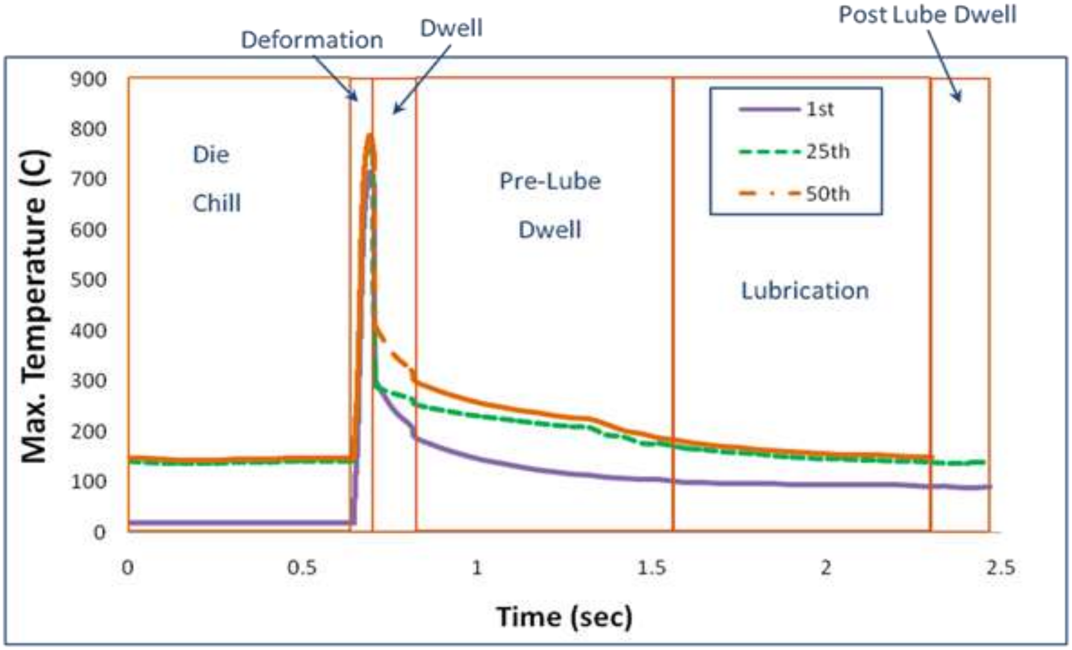

Figure 17: Maximum Temperature in the Extrusion Die during the 1st, 25th, and 50th Cycle [Deshpande et. al., 2009]

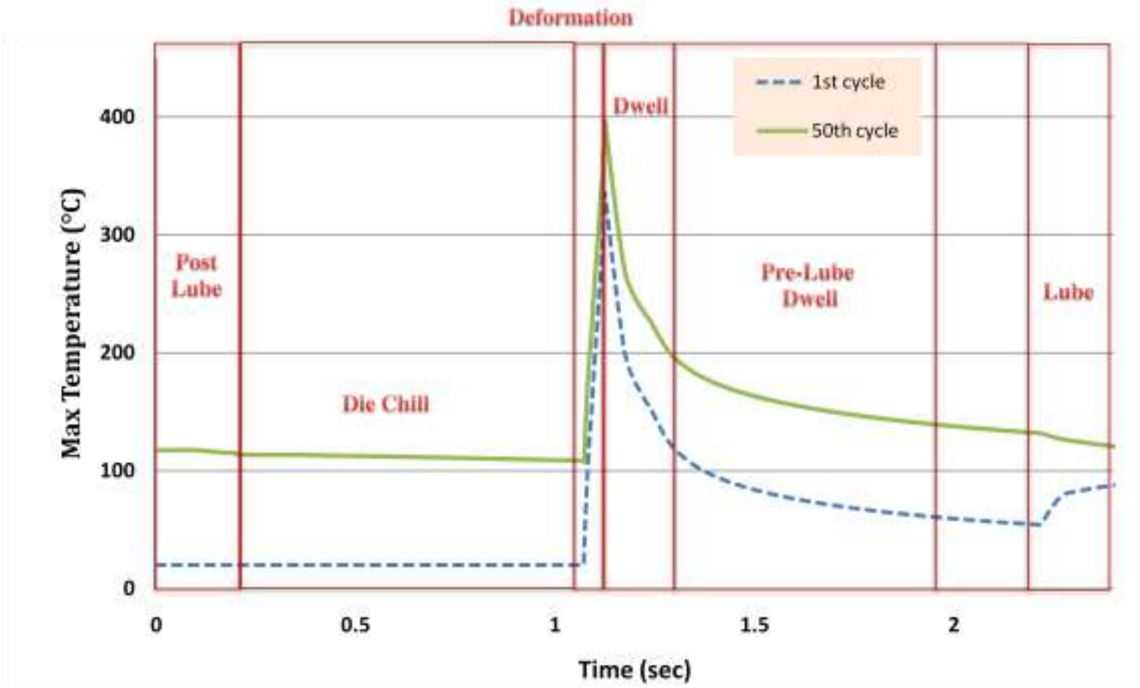

Figure 18: Maximum Temperature in the Coining Die during the 1st and 50th cycle [Deshpande et. al., 2009]

As seen with the pinion shaft, the die temperatures at the end of the cycle are higher than at the start. The next cycle is started with the temperature distributions from the previous cycle. This process was continued for 50 cycles and the steady state temperature distributions are shown in Figure 19 (extrusion) and Figure 20 (coining).

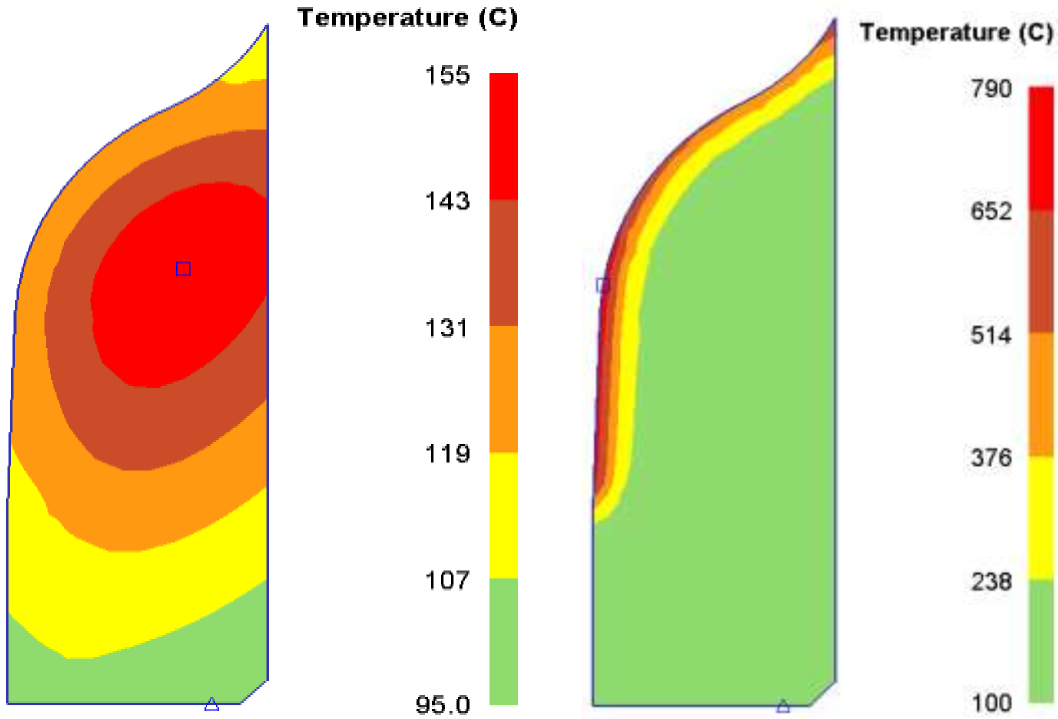

(a) At the start of cycle

(b) After deformation

Figure 19: Steady State Temperature Distribution of Extrusion Die for the 50th Cycle [Deshpande et. al., 2009]

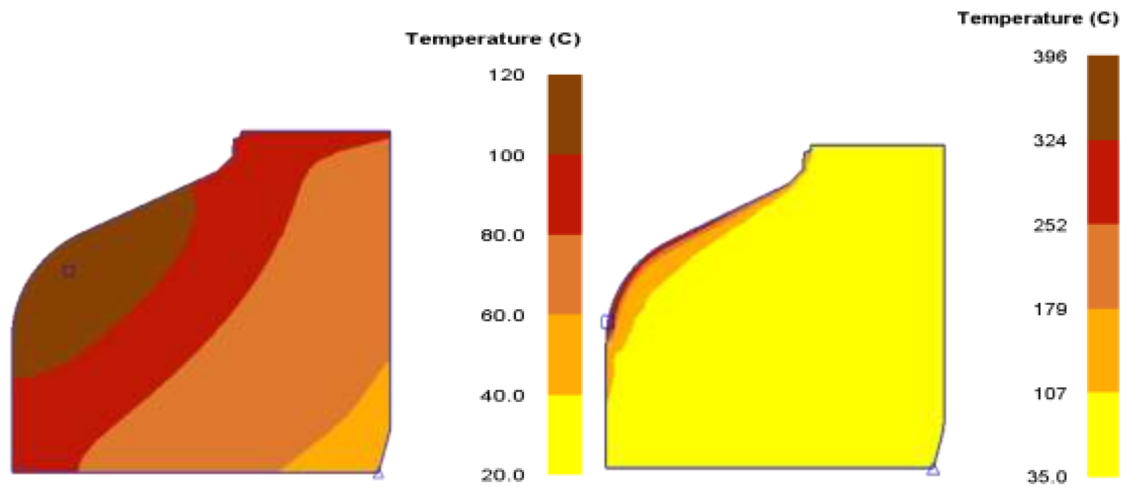

(a) At the start of cycle (b) After deformation

Figure 20: Steady State Temperature Distribution of Coining Die for the 50th Cycle [Deshpande et. al., 2009]

Prediction of Plastic Deformation of Die

The plastic deformation was estimated for the extrusion die, as it was for the pinion shaft extrusion die. A series of FEA simulations was performed using a flow stress model, which was formulated based on the material data provided by the tool steel manufacturer. However, the plastic deformation and subsequent wear analysis was only performed for the extrusion die and not the coining die. This was due to the fact that the coining die was not seen to have been failing with extreme wear. Therefore, the following discussion is only pertaining to the extrusion die.

The procedure is the same as for the pinion shaft. The simulation for plastic deformation is summarized below.

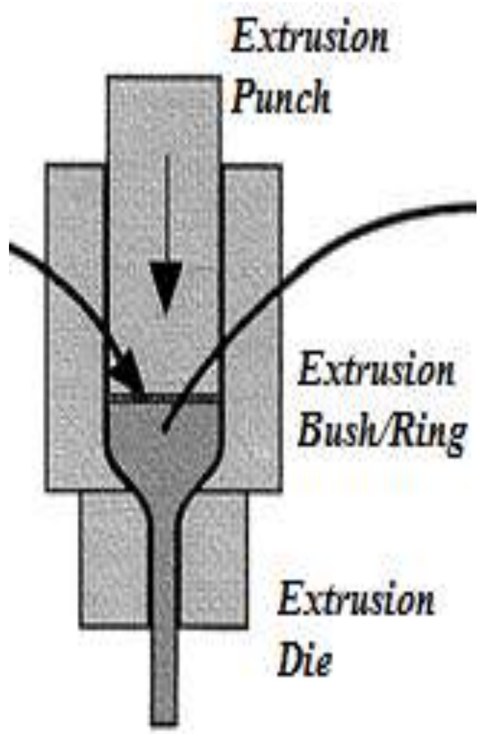

Figure 21: Schematic of Extrusion Tooling [Deshpande et. al., 2009]

The results for the simulations are shown in Figure 22. The elastic and plastic deformation (during the deformation process of extruding the valve) of the die is shown by the dashed line and labeled ‘after deformation’. The plastic deformation after all loads have been removed (mechanical and thermal loads) is illustrated in the dashed-dot line, labeled ‘after die cooling’. The solid line shows the die deflections due to elastic and thermal loads (excluding the plastic deformation) and is labeled ‘before deformation’.

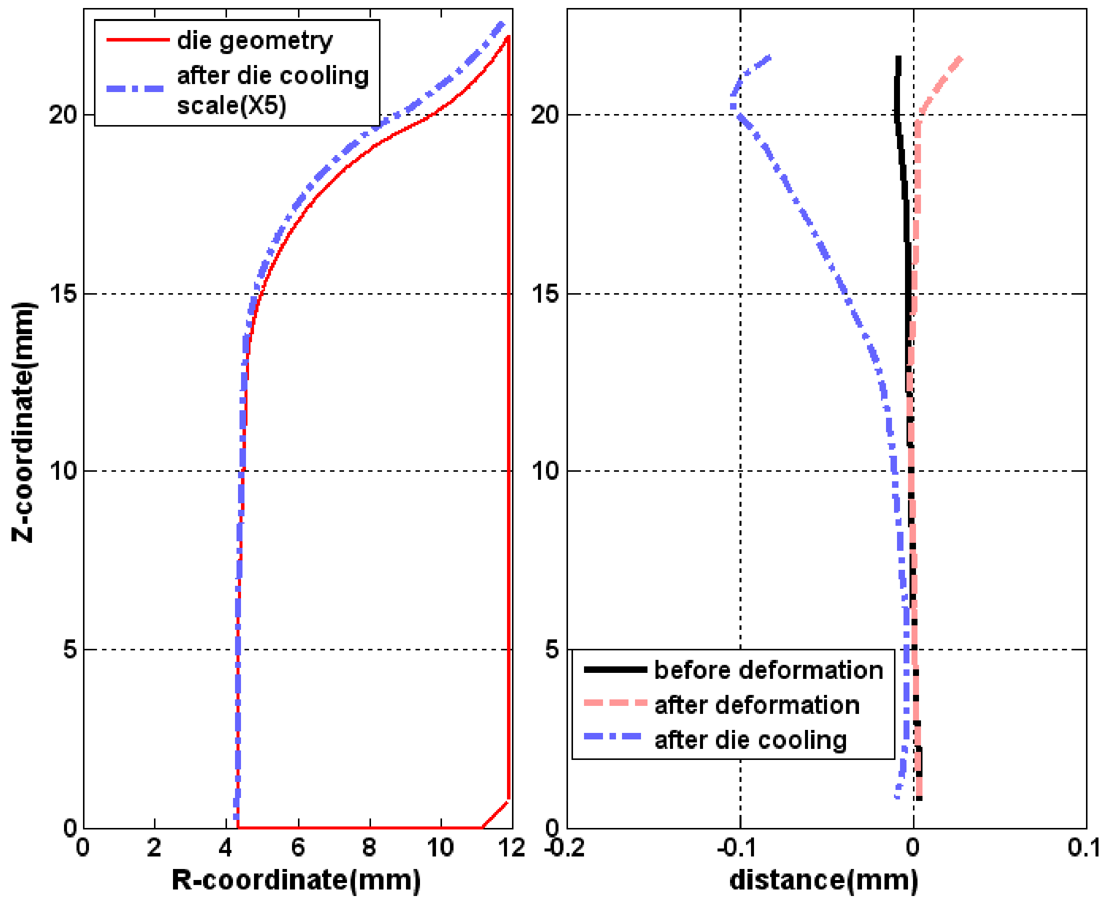

Figure 22: Initial Die Geometry and Plastic Deformation (left) and Deformation of the Die (right), Elastic and Plastic Deformation including Thermal Deflections (dashed line) and the Plastic Deformation (dashed-dot line), Elastic and Thermal Deflections excluding Plastic Deformation (solid line)

Prediction of Abrasive Die Wear

The abrasive wear for the valve extrusion die is performed similarly to the pinion shaft analysis. The results are shown in Figure 23 for the average pressure and velocity with respect to the location on the die surface.

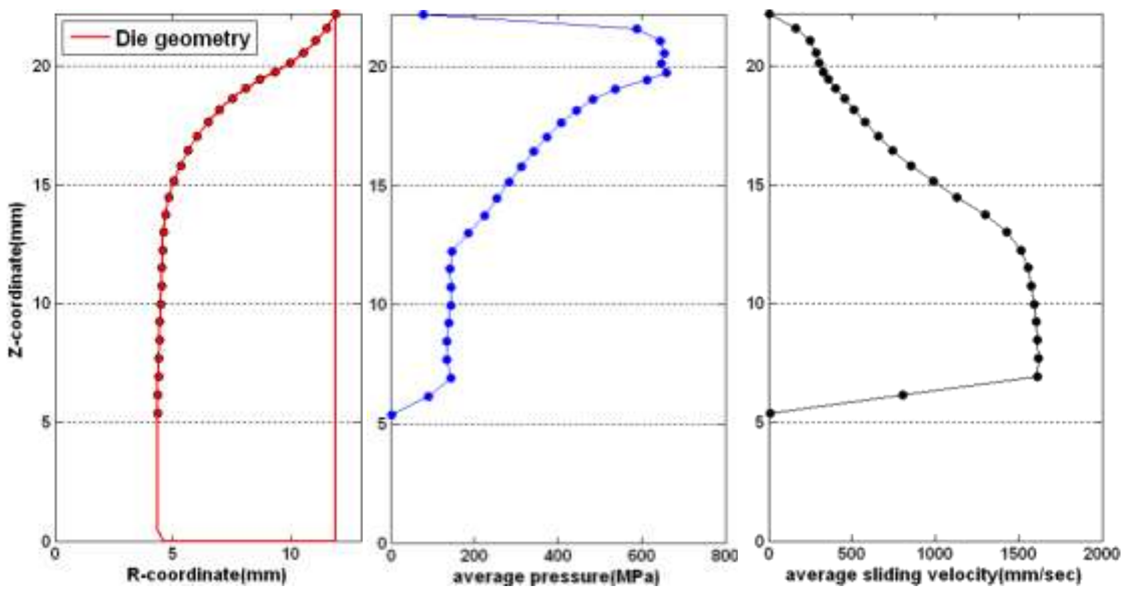

Figure 23: Average Pressure (middle) and Sliding Velocity (right) versus the location on the Die Surface (left)

Chapter 5: Comparison of FEA with Experiments

Production runs for both case studies were used for experimental data. Experimentally used dies were measured and analyzed to confirm the FEA results. The experimental dies were cut into half-sections and measured on a Coordinate Measurement Machine (CMM) to obtain the "worn" profile. In reality, the measured profile is a combination of wear and plastic deformation, which is why the plastic deformation was predicted earlier. The properties of the measured dies, for the pinion shaft, are given in Table 3.

	Case Study 1- Pinion Shaft			
Property	**Extrusion Insert A (Not Studied)**	**Extrusion Insert B**	**Extrusion Insert C**	**Extrusion Insert D (Not Studied)**
Material	DURO-F1	DURO-F1	DURO-F1	DURO-F1
Hardness of Base Metal	59 HRC	59 HRC	59 HRC	59 HRC
Nitride Depth (and Hardness)	0.22 mm (70 HRC)	0.22 mm (70 HRC)	0.22 mm (70 HRC)	0.22 mm (70 HRC)
Number of Cycles (Life)	2,200	1,800	3,100	13,300

Table 3: Pinion Shaft Extrusion Die Properties

Though some of the dies were not evaluated in the wear study, their properties are given in the tables. For the pinion shaft, Extrusion Inserts B and C were chosen to be evaluated because their "worn" profiles were similar and there was a small difference between die life (1800 and 3100 cycles, respectively). Extrusion Insert A was not studied because its “worn” profile was seen to have too much error in the measurement. Extrusion Insert D was not studied for wear because it failed due to fracture and not wear. Also failing due to fracture and not wear, two other dies were not presented in this research. One die of DRM-1 and one of DRM-2 cracked after 15000 and 9100 cycles, respectively.

The engine valve coining die was also not studied for die wear. This was because it lasted about four times as long as the extrusion die and did not have the same extreme amounts of wear.

Die Profile Measurements

The Sheffield Cordax CMM which was used to measure the wear profile is a touch probe type CMM in which a probe comes in contact of the work piece to locate the point being measured. The radius of the probe was 1 mm. Touch probe radius compensation was used to get the exact location of the points where the probe comes in contact with the workpiece. [Deshpande et. al., 2009]

The die profile measurement is explained using the extrusion die as an example in Figure 24. Due to small size, requirement of surface measurement of the die profile and limited surfaces to affix the die, it was not able to be clamped on the CMM table using regular clamps or bolts. The die was held using a magnet onto a block which was further attached to the CMM table using bolts. It was assumed that the magnet can sufficiently attract the workpiece so that there is no movement of the die during the measurement of the profile. [Deshpande et. al., 2009]

Only some part of the bottom surface of the die was used to attach the magnet as the rest of the bottom surface was used as a reference plane for further measurements. The block was used to raise the die sufficiently enough for the probe to measure the bottom surface. [Deshpande et. al., 2009]

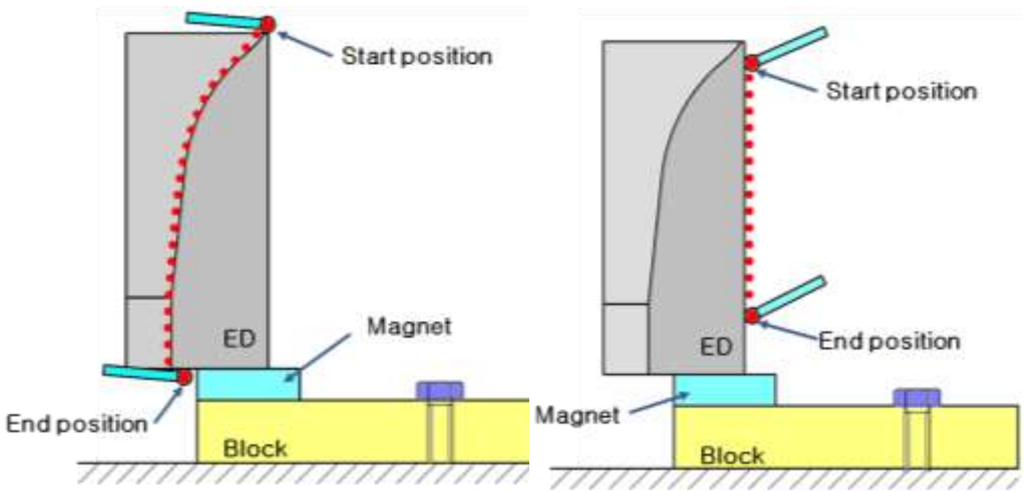

(a) Measure the inside profile (b) Measure the outside profile

Figure 24: Arrangement of Die on CMM Table [Deshpande et. al., 2009]

As the wear and plastic deformation on the die surface may or may not be symmetric about the vertical axis of the die, three profile lines were measured which were later processed using Matlab to get an average inner profile. To get the vertical axis of the part, four outer profile lines were used to fit an average vertical axis for the die. The measured points on the extrusion die are shown in Figure 25. [Deshpande et. al., 2009]

The distance interval between every point measured on the CMM were 0.09mm and 0.11mm for the inner profile and outer profile, respectively. [Deshpande et. al., 2009]

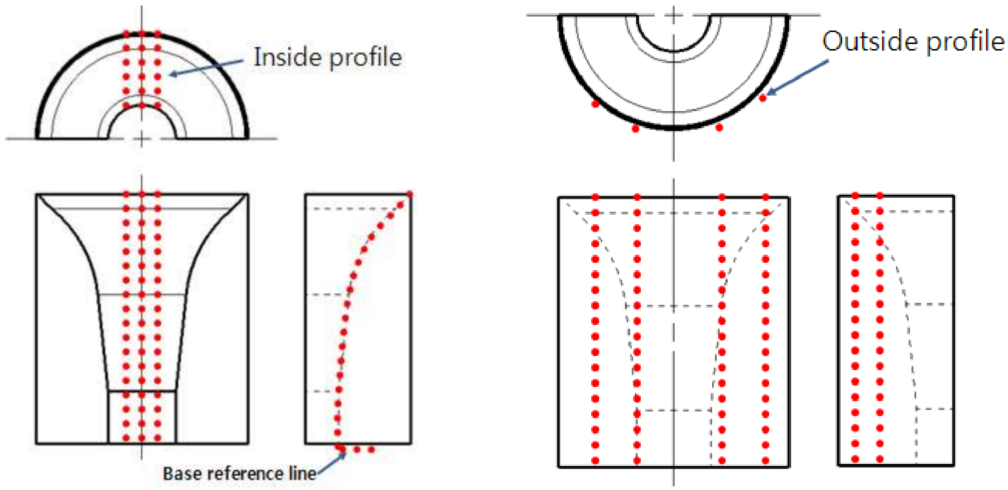

(a) Measure the inside profile

(b) Measure the outside profile for find center line

Figure 25: Measured Points for the Profile of the Extrusion Die [Deshpande et. al., 2009]

The CMM data collected is in the form of coordinates of the points where the CMM touch probe comes in contact with the dies. The four outer profiles generated using CMM are used to fit a single vertical axis to the die. The three inner profile lines are measured in three different vertical planes, hence it was necessary to convert the three dimensional data (XYZ coordinate) into two dimensions (RZ coordinates), such that the origin is located (where the central vertical and the base line of the dies meet). [Deshpande et. al., 2009]

After converting the three inner die profiles from XYZ coordinate into RZ coordinate, an average inner profile is generated. This average inner profile is compared with the original geometry of the die to get the horizontal deviations at any position on the die surface. The measured die profiles for the extrusion die (scale = 5X) is shown in Figure 26. [Deshpande et. al., 2009]

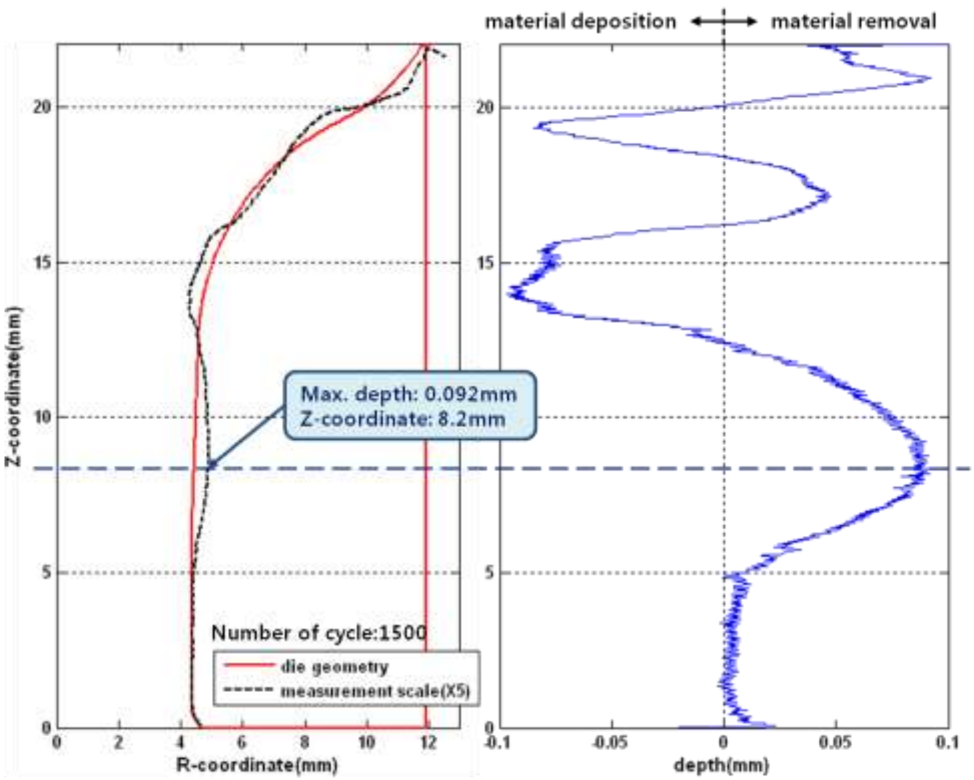

Figure 26: Plot Showing the Original Die Geometry and Measured Real Die "Wear" Profile of Extrusion Die [Deshpande et. al., 2009]

Case Study 1- Steel Pinion

As discussed before, the plastic deformation was predicted and is shown in Figure 27, as the solid line in the right side graph. The results of the CMM measurements are in Figure 28, for both Extrusion Insert B and C (1800 cycle and 3100 cycle, respectively). It can be seen that the measured data has a tilt that is similar to the tilt in the plastic deformation prediction. This is because the CMM measurement includes the plastic deformation.

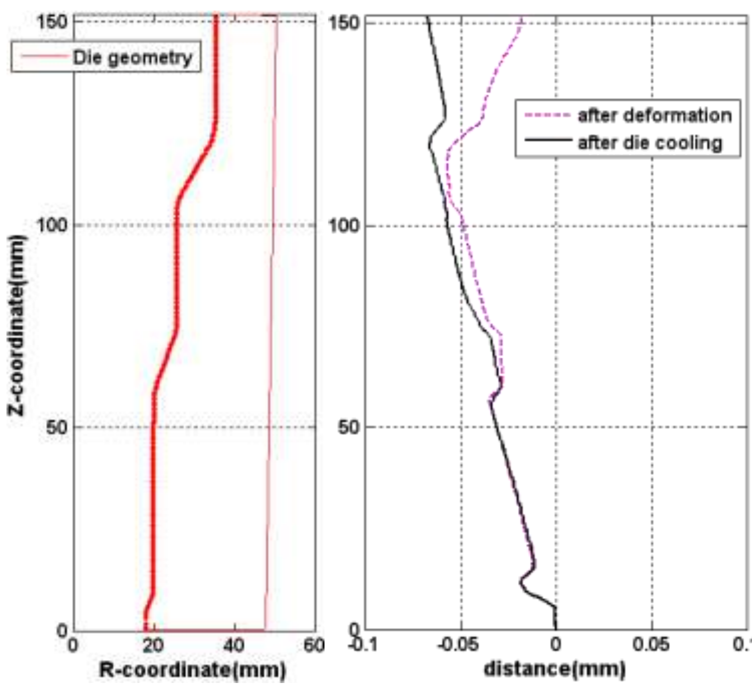

Figure 27: Initial Die Geometry (left) and Deformation of the Die (right), Elastic and Plastic Deformation including Thermal Deflections (dashed line) and the Plastic Deformation (solid line)

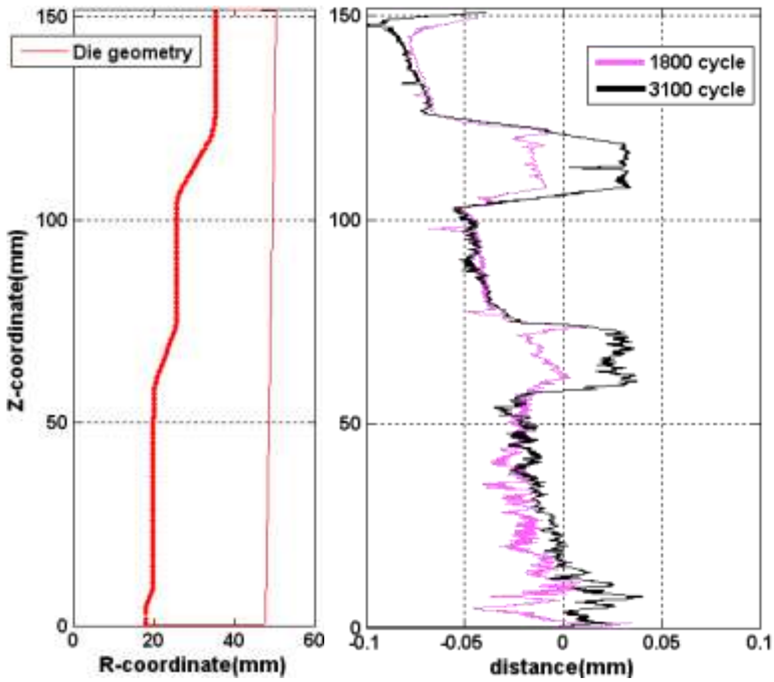

Figure 28: CMM Measurement Results for Extrusion Inserts B and C

In Figure 29, the predicted plastic deformation (‘plastic deformation’) is compared to the CMM measurements (‘measured wear depth’) for Extrusion Insert B (1800 Cycles). Using the plastic deformation (dashed line) as the zero axis upon which the CMM data is compared, the wear can be quantified. The CMM data for Extrusion Insert B and C is shifted so that the zero axis (plastic deformation geometry) is the vertical axis at zero (Figure 30). Figure 30 shows that most of the CMM data is to the right of the zero axis and therefore, is wear. Using the wear profile and the FEA simulation results (velocity, pressure, time, temperatures), as well as the hot hardness, the wear equation can be applied and the experimental constants (K and a) can be determined. Figure 31 and 32 show the simulation results and hot hardness values used to determine the wear equation constants.

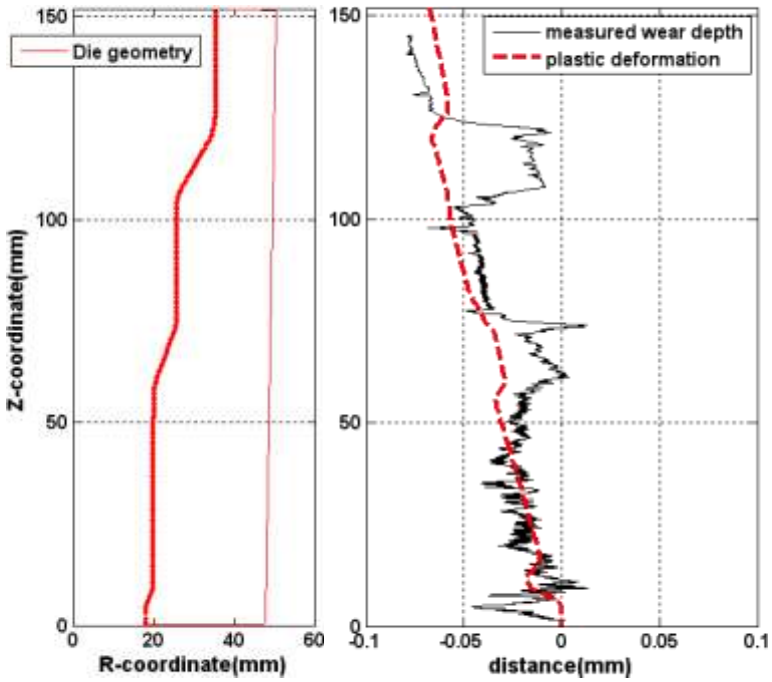

Figure 29: Predicted Plastic Deformation versus CMM Measurement for Extrusion Insert B (1800 Cycles)

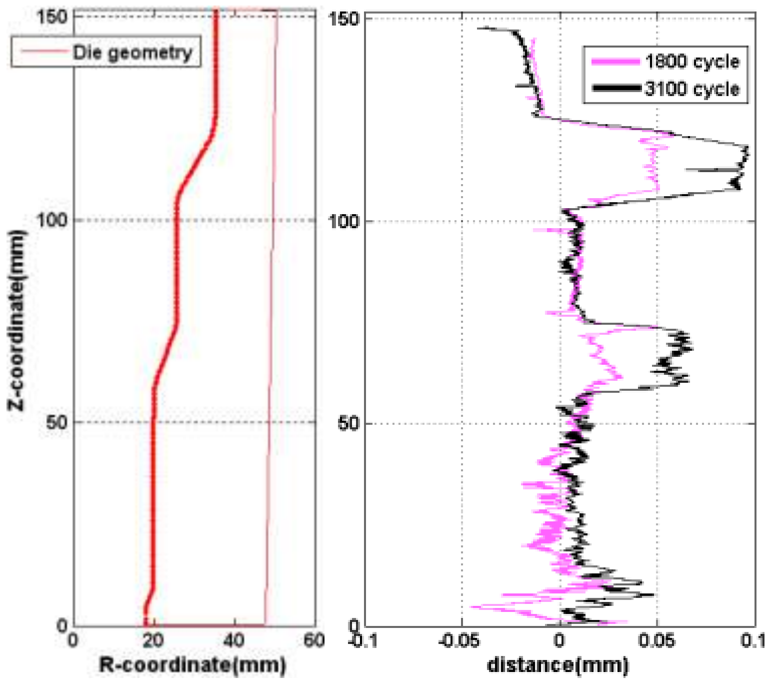

Figure 30: Corrected CMM Data to Account for Plastic Deformation

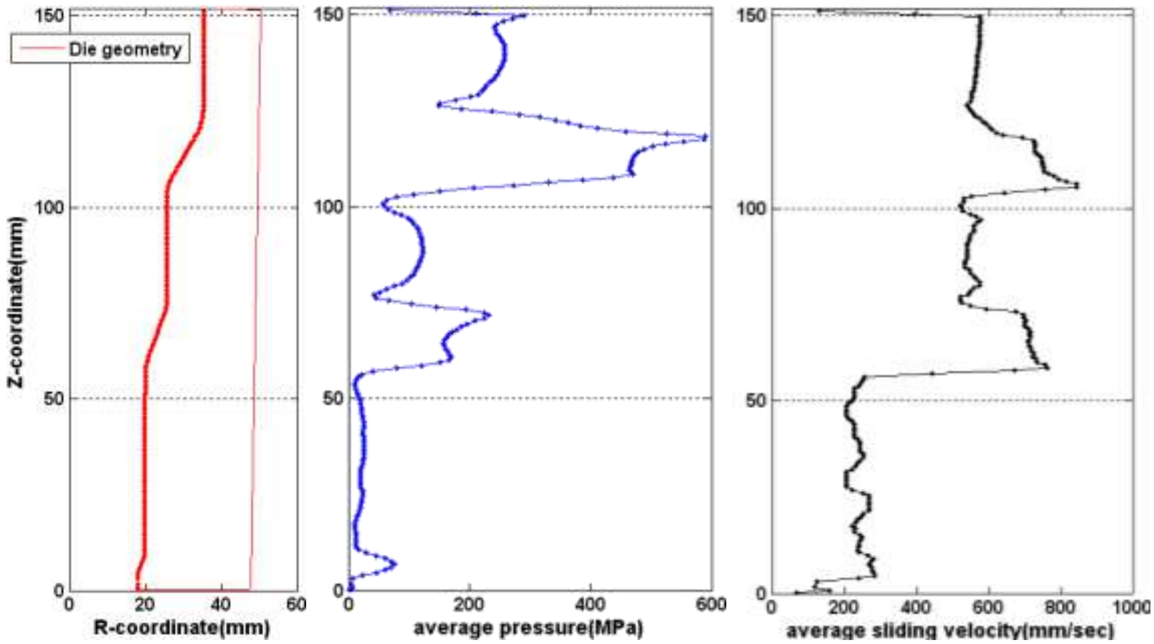

Figure 31: Average Pressure (middle) and Sliding Velocity (right) versus the Location on the Die Surface (left)

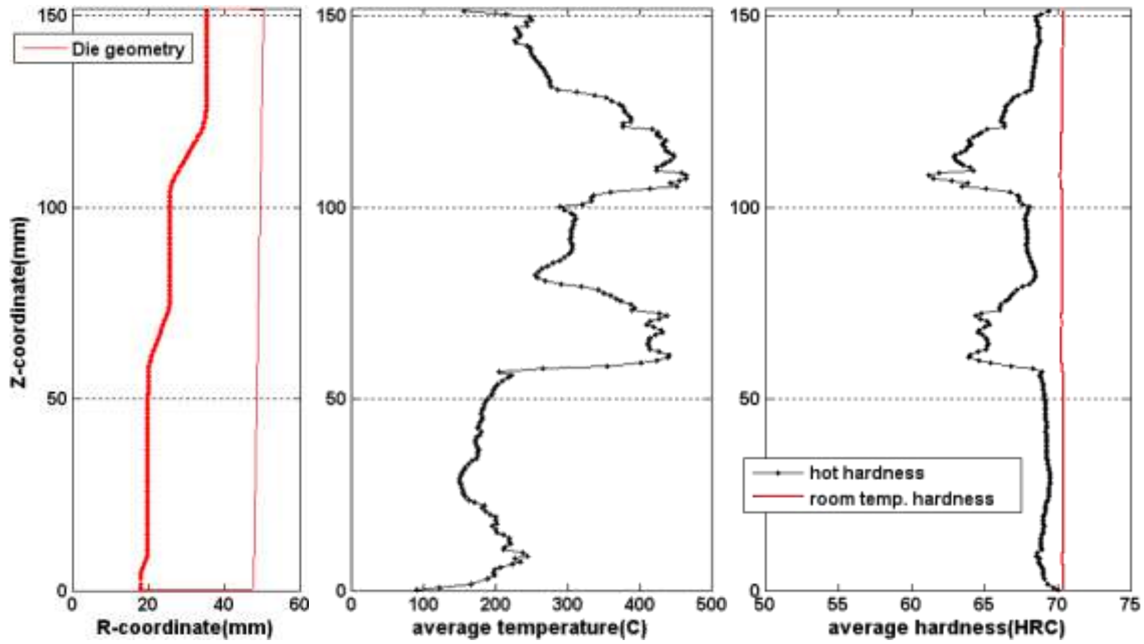

Figure 32: Average Temperature (middle) and Hot Hardness (right) versus the Location on the Die Surface (left)

A sensitivity analysis of the experimental constant ‘*a*’ was performed (Figure 33). It can be seen that ‘a’ affects the shape of the predicted wear, while ‘*K*’ affects the magnitude (as a constant coefficient).

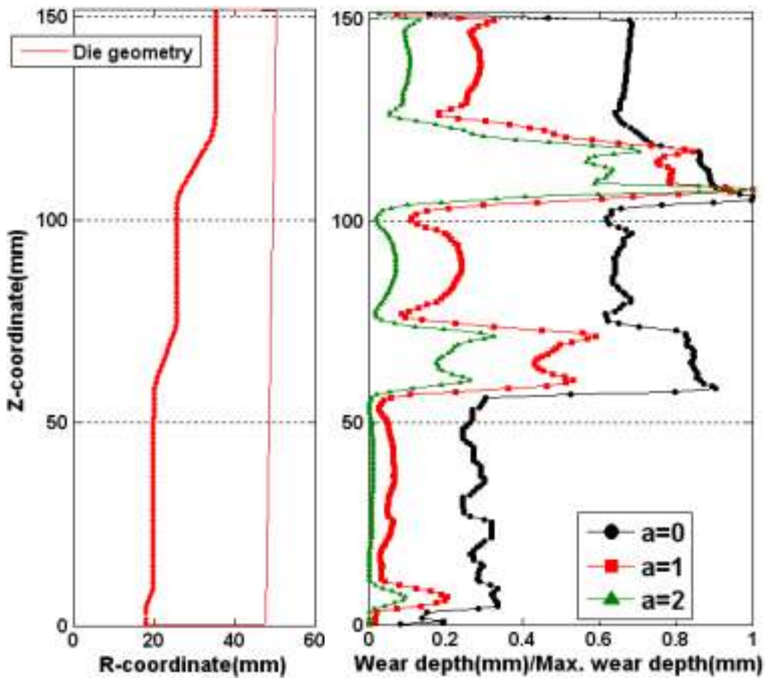

Figure 33: Sensitivity Analysis for Experimental Constant ‘a’

Using Matlab, the experimental constants ‘K’ and ‘a’ are optimized to give a minimum error between the predicted wear value (through the equation) and the actual wear value (from the CMM data compensated for plastic deformation). Figure 34 shows the optimization curves and Table 4 lists the final values of the optimization.

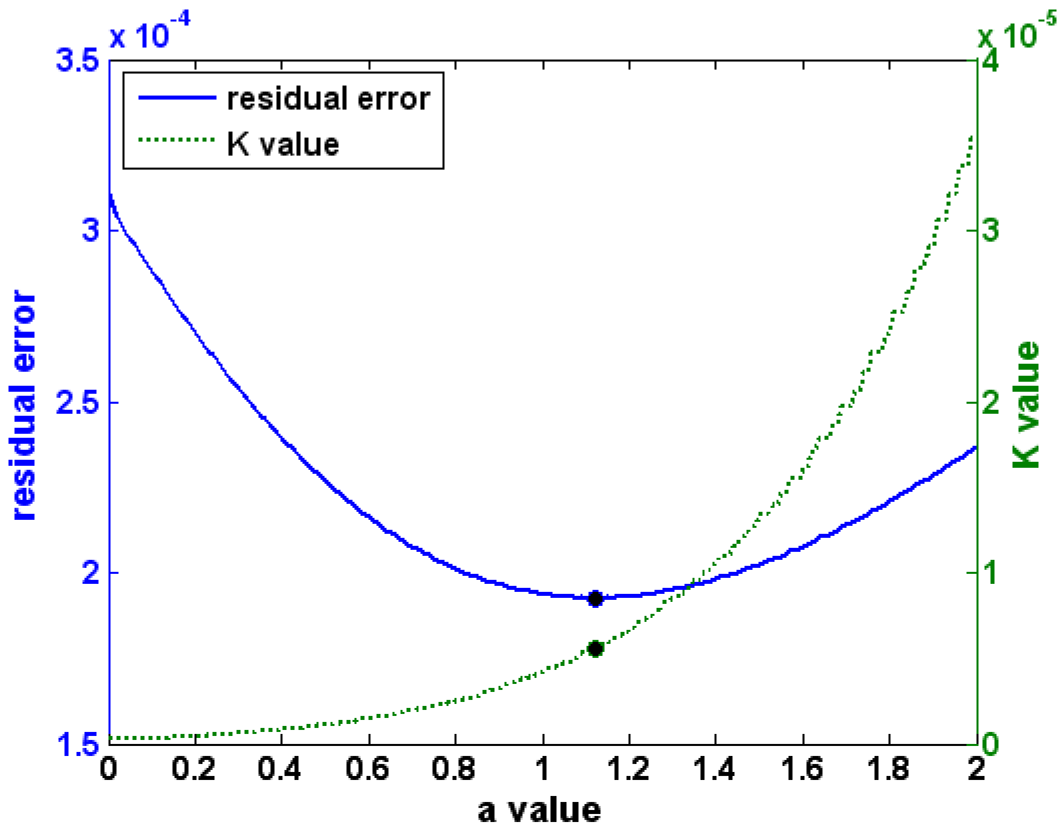

Figure 34: Optimization Curves for Experimental Constants ‘K’ and ‘a’

Optimized value	
K	**5.543 E-6**
a	**1.12**
error	**1.925 E-4**

Table 4: Optimization Results for Wear Equation Constants

The predicted wear, from the FEA simulation and wear equation results, is compared to the measured wear data, from the CMM measurements modified for plastic deformation, in Figure 35. The comparison shows that the prediction is very close to the input information (as it should be).

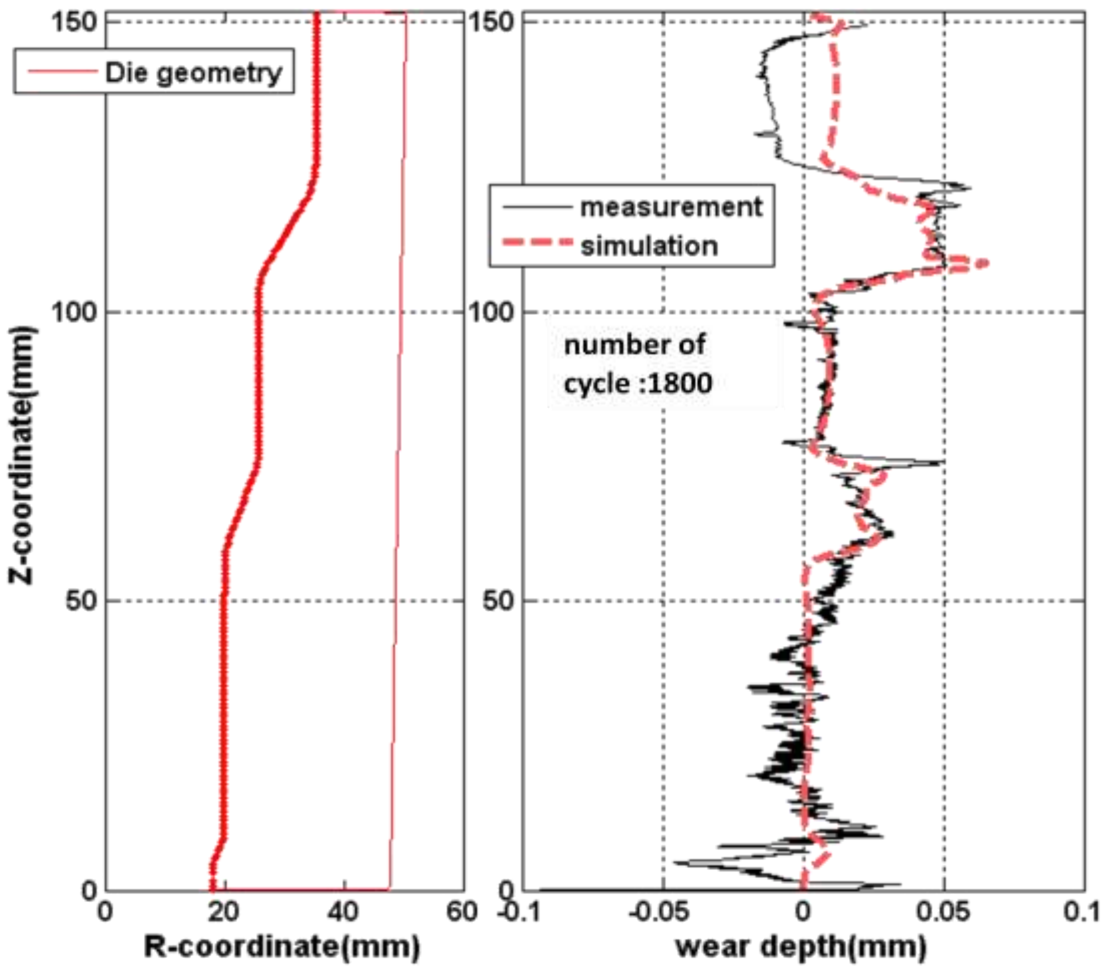

Figure 35: Predicted Wear (Combined Simulation and Wear Equation Results) (‘simulation’) versus CMM Measured Wear (Compensating for the Plastic Deformation) (‘measurement’) for Extrusion Insert B (1800 Cycles)

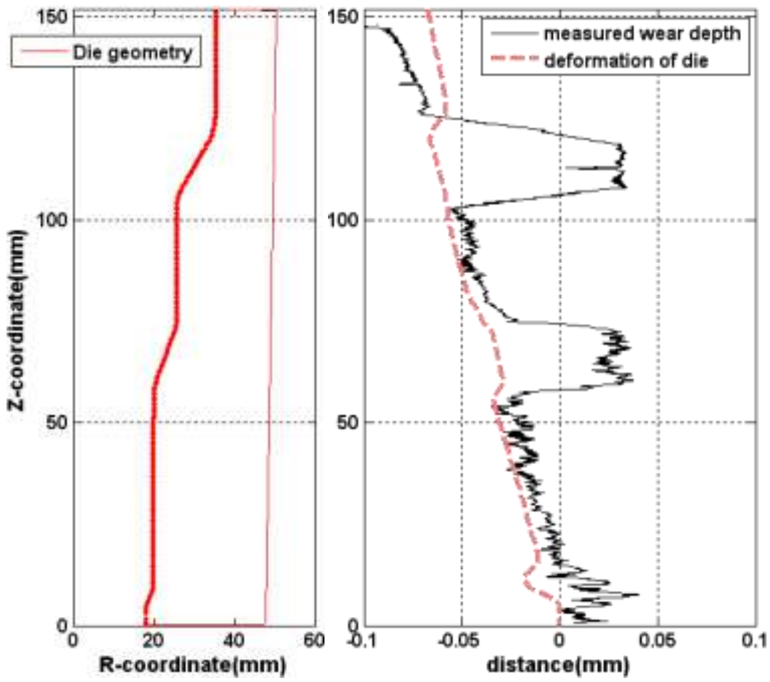

Figure 36: Predicted Plastic Deformation versus CMM Measurement for Extrusion Insert C (3100 Cycles)

For Extrusion Insert C, the plastic deformation results for 3100 cycles versus the CMM data is shown in Figure 36. The figure illustrates a similar tilt as seen with Extrusion Insert B and 1800 cycles. The results for the wear equation constants ('*K*' and '*a*') from the 1800 cycle example are now applied to the 3100 cycle die example. Using these results, a predicted wear profile is determined and compared with the measured profile, after compensating for plastic deformation (Figure 37). The prediction matches the actual wear very well, in location as well as in magnitude.

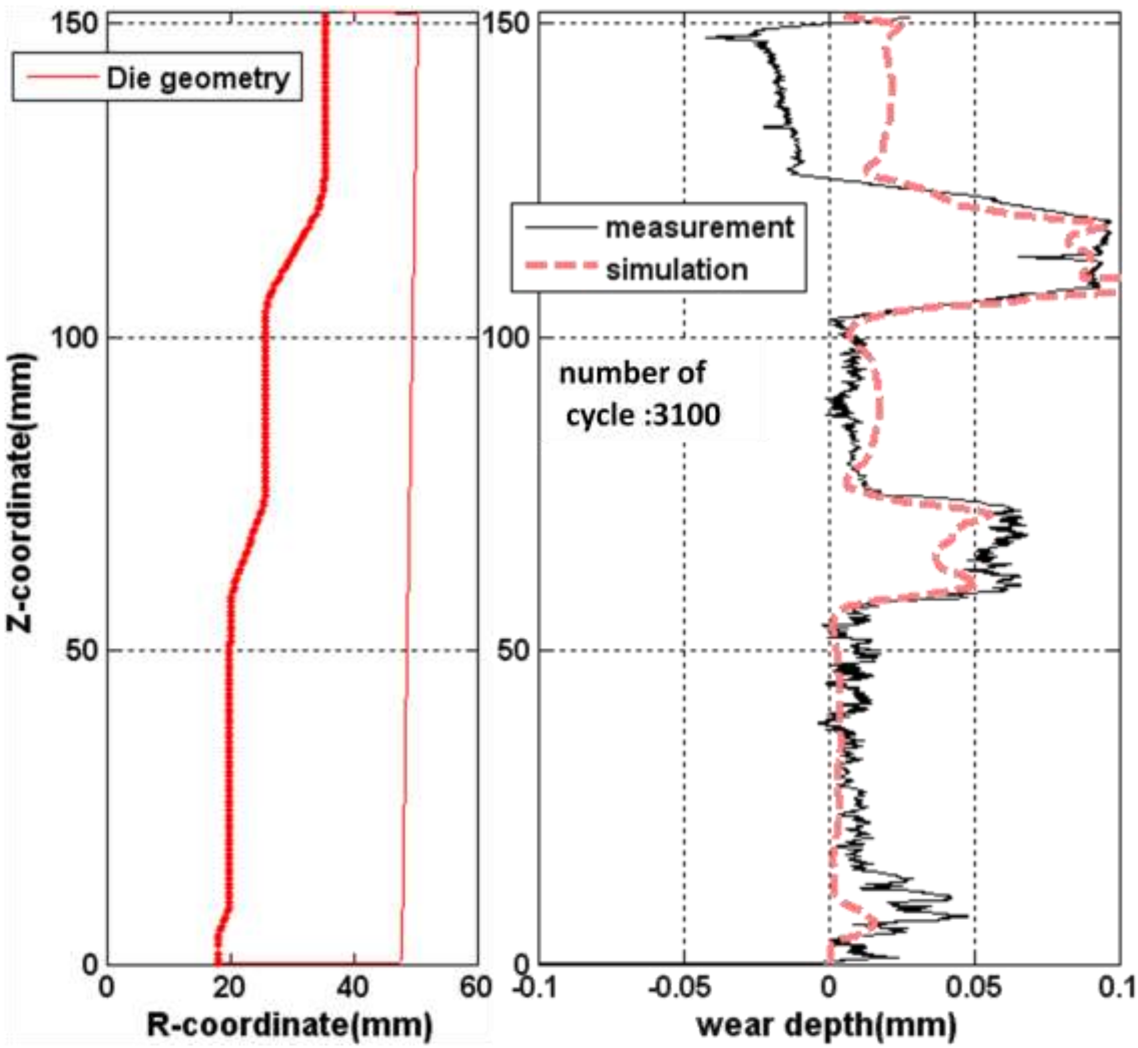

Figure 37: Predicted Wear (Combined Simulation and Wear Equation Results) (‘simulation’) versus CMM Measured Wear (Compensating for the Plastic Deformation) (‘measurement’) for Extrusion Insert C (3100 Cycles)

The plastic deformation was predicted and is shown in Figure 38, as the dashed-dot line in the right side graph, as shown before. The results of the CMM measurements are in Figure 39, for the Extrusion Die.

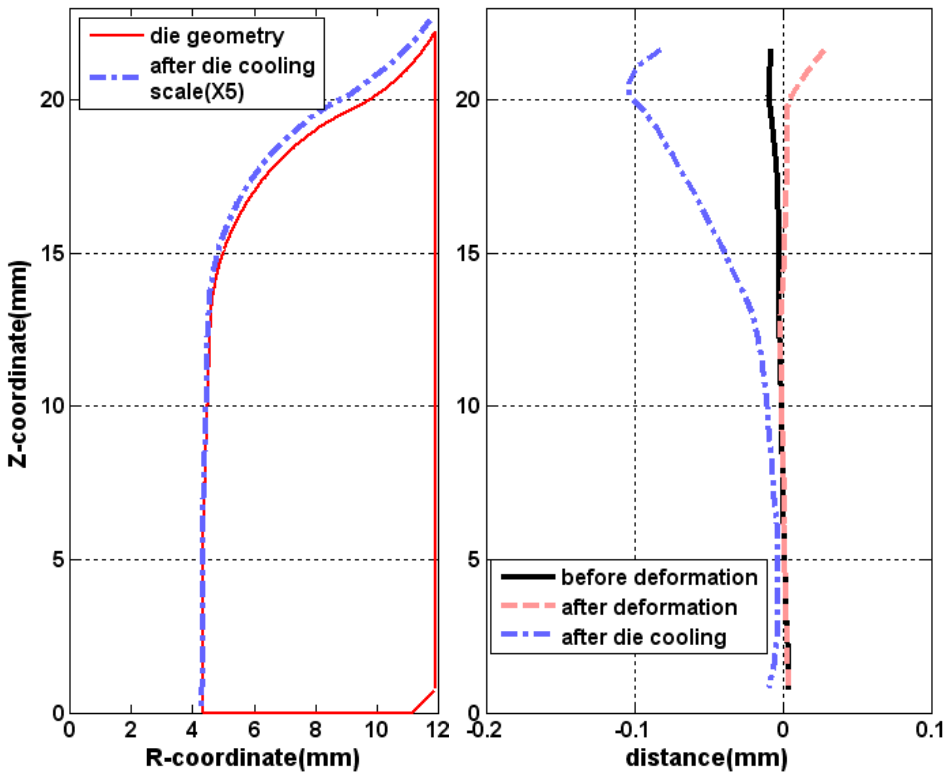

Figure 38: Initial Die Geometry and Plastic Deformation (left) and Deformation of the Die (right), Elastic and Plastic Deformation including Thermal Deflections (dashed line) and the Plastic Deformation (dashed-dot line), Elastic and Thermal Deflections excluding Plastic Deformation (solid line)

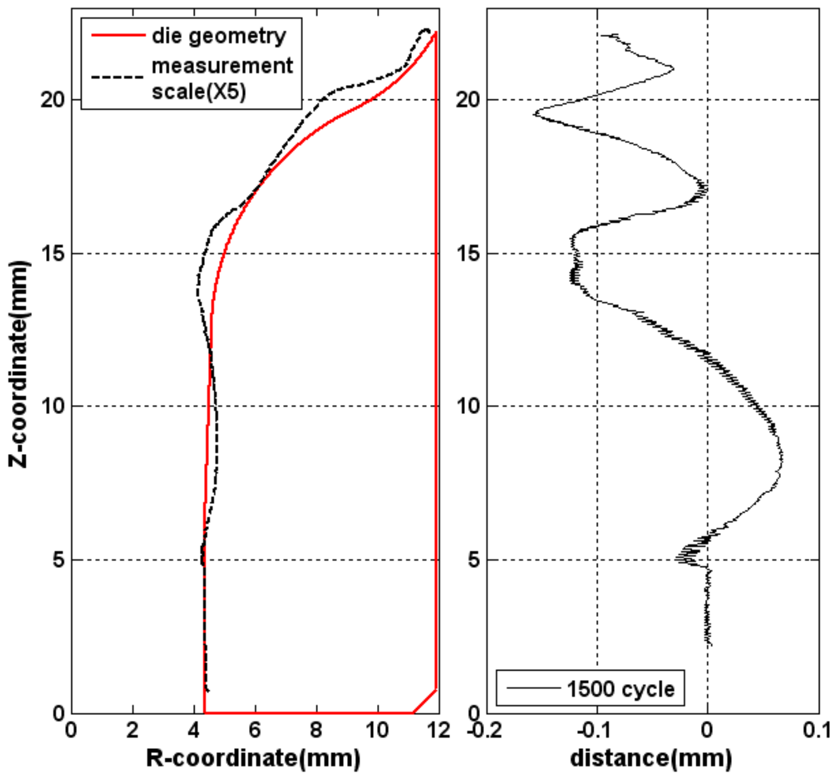

Figure 39: CMM Measurement Results for Extrusion Die

In Figure 40, the predicted plastic deformation (‘deformation of die’) is compared to the CMM measurements (‘measured wear depth’) for the Extrusion Die. Using the plastic deformation (dashed-dot line) as the zero axis upon which the CMM data is compared, the wear can be quantified. The CMM data for the Extrusion Die is shifted so that the zero axis (plastic deformation geometry) is the vertical axis at zero (Figure 40, on the right). Figure 40 also shows that the CMM data is both to the left and right of the zero axis and therefore, cannot be considered only wear. Using the “wear” profile (assumed from the previous step, though not correct) and the FEA simulation results (velocity, pressure, time, temperatures), as well as the hot hardness, the wear equation can be applied and the experimental constants (*K* and *a*) are determined. Figure 41 and 42 show the simulation results and hot hardness values used to determine the wear equation constants.

A sensitivity analysis of the experimental constant '*a*' was also performed (Figure 43). It can be seen that '*a*' affects the shape of the predicted wear, while '*K*' affects the magnitude (as a constant coefficient), as before with the pinion shaft.

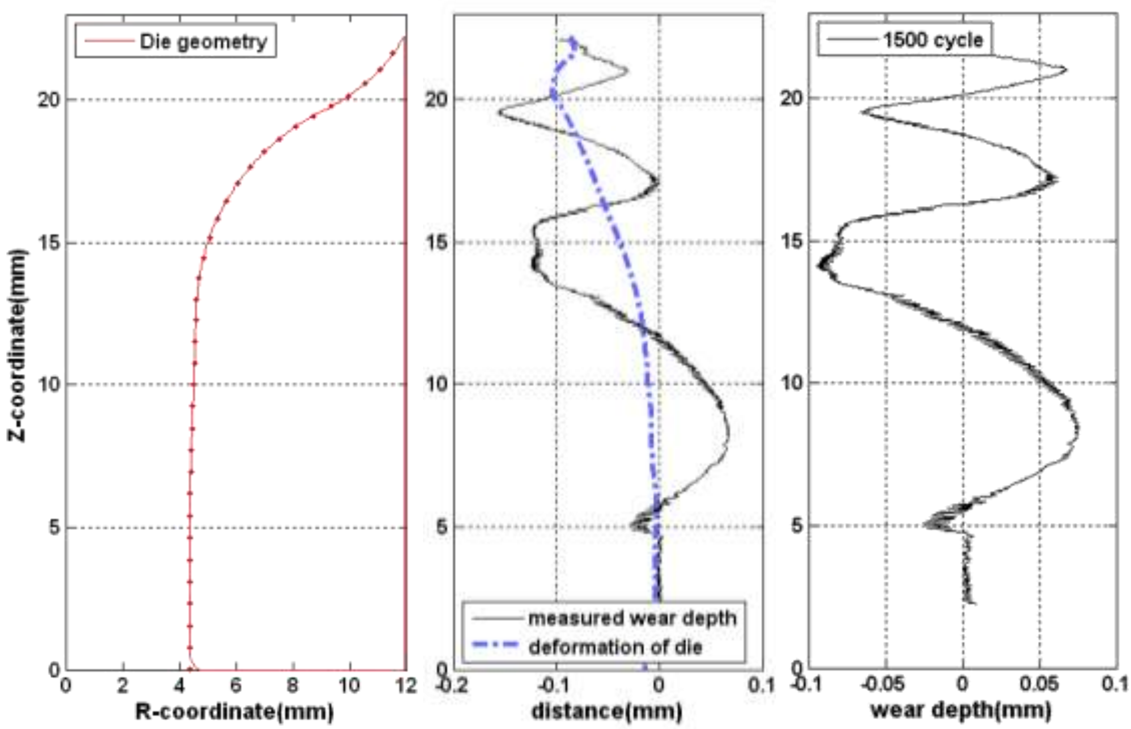

Figure 40: Predicted Plastic Deformation versus CMM Measurement for Extrusion Die (middle) and Corrected CMM Data to Account for Plastic Deformation (right)

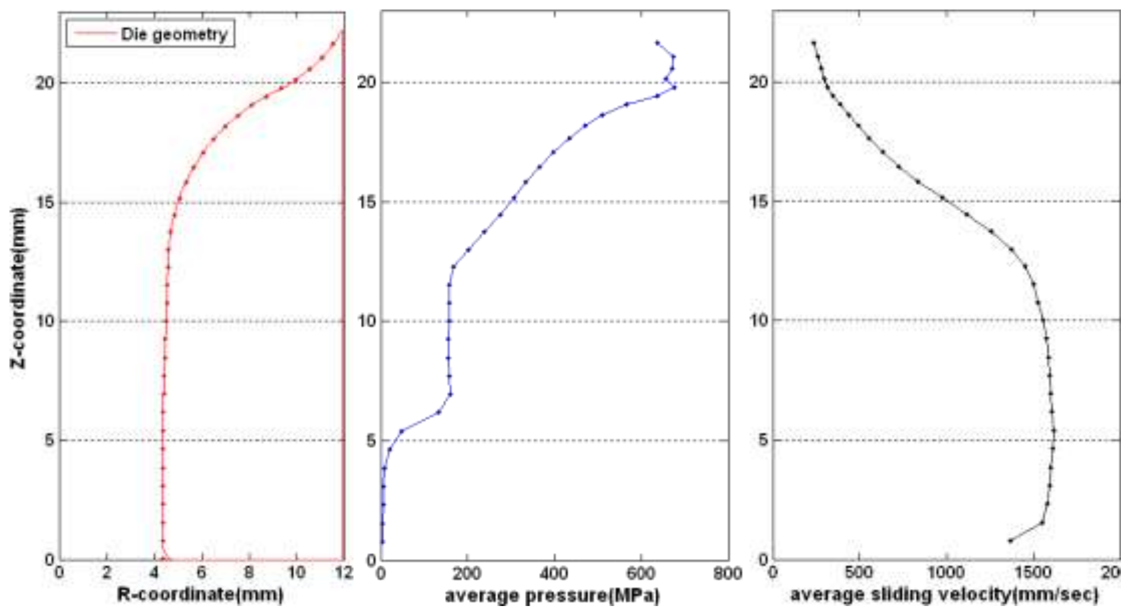

Figure 41: Average Pressure (middle) and Sliding Velocity (right) versus the Location on the Die Surface (left)

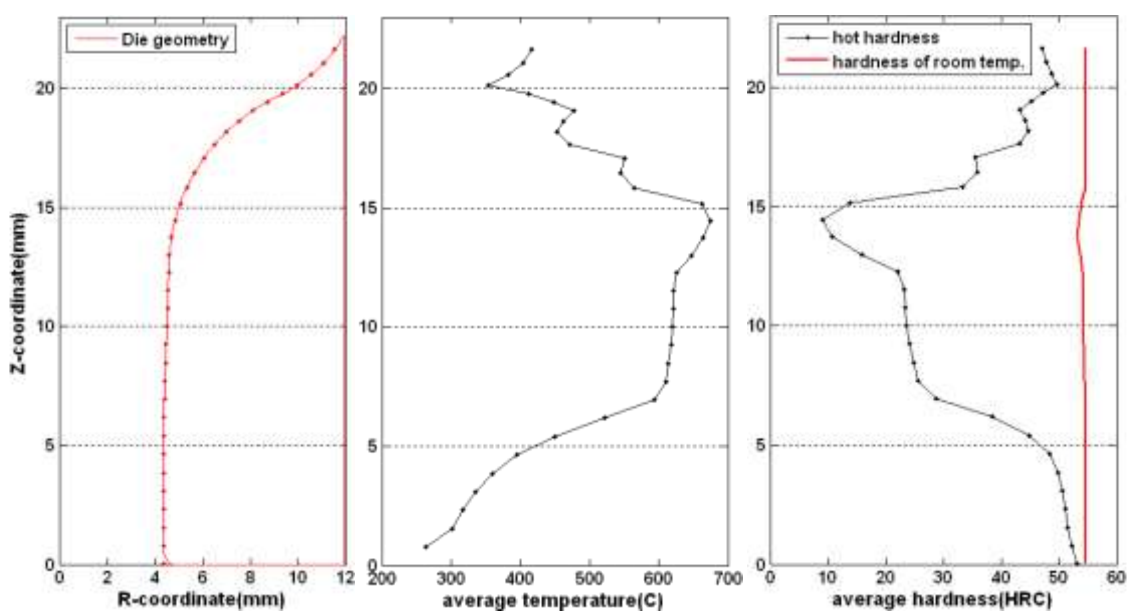

Figure 42: Average Temperature (middle) and Hot Hardness (right) versus the location on the Die Surface (left)

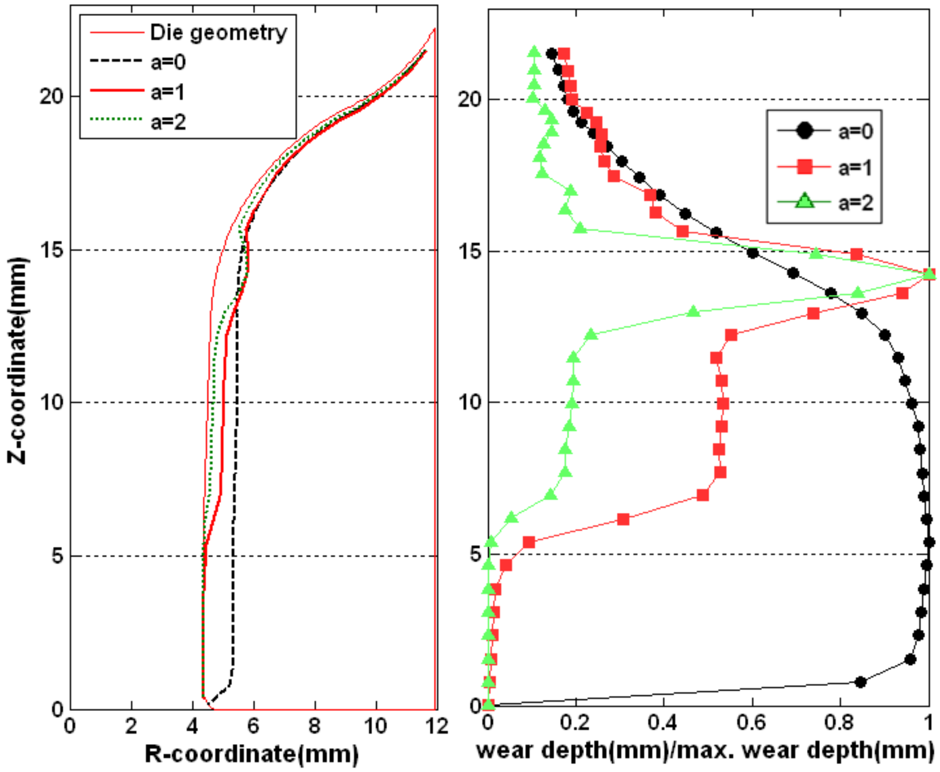

Figure 43: Sensitivity Analysis for Experiment Constant 'a'

Using Matlab as before, the experimental constants ‘K’ and ‘a’ are optimized to give a minimum error between the predicted wear value (through the equation) and the actual wear value (from the CMM data compensated for plastic deformation). Figure 44 shows the optimization curves and Table 5 lists the final values of the optimization.

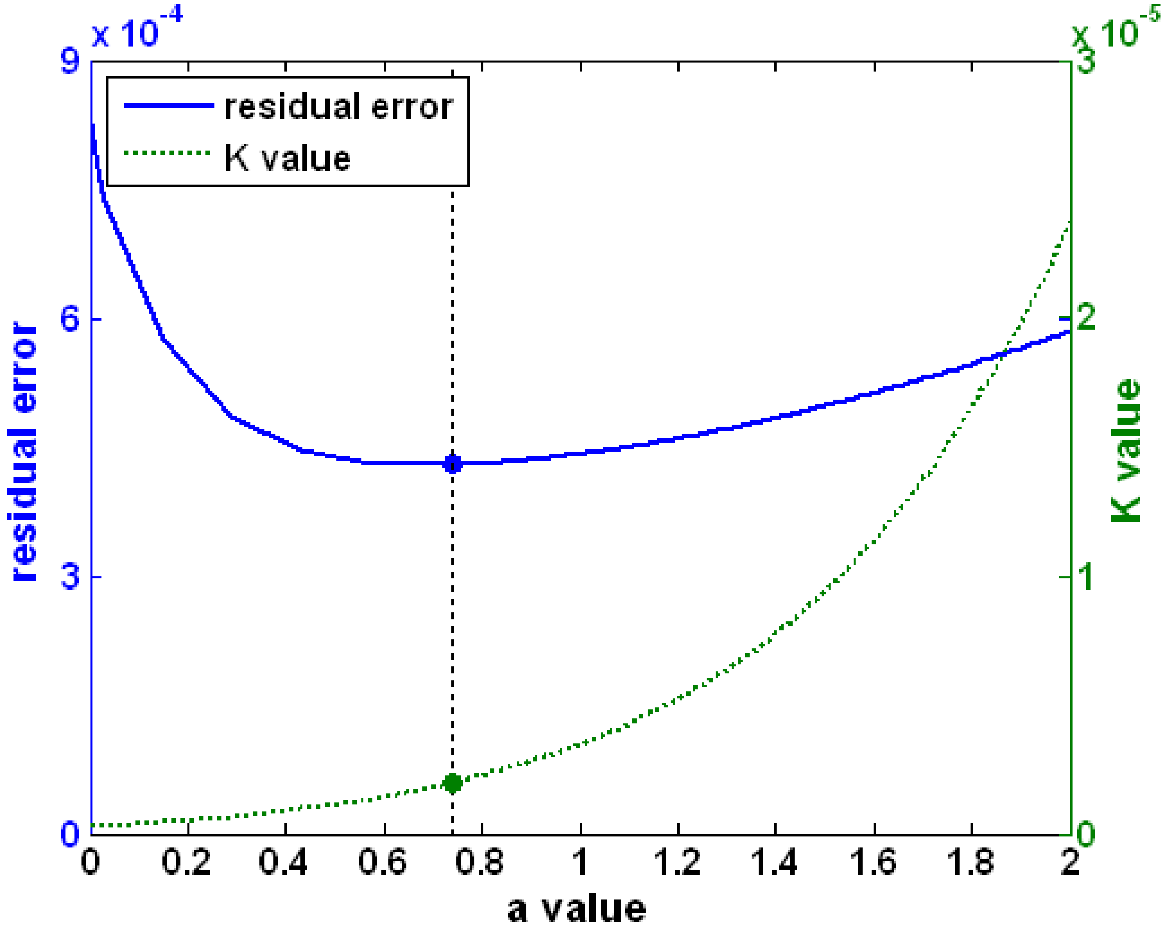

Figure 44: Optimization Curves for Experimental Constants 'K' and 'a'

Optimized value	
K	**2.00 E-6**
a	**0.74**
error	**3.422 E-4**

Table 5: Optimization Results for Wear Equation Constants

The predicted wear, from the FEA simulation and wear equation results, is compared to the measured wear data, from the CMM measurements modified for plastic deformation, in Figure 45. The comparison shows that the prediction is not in agreement with the measurement.

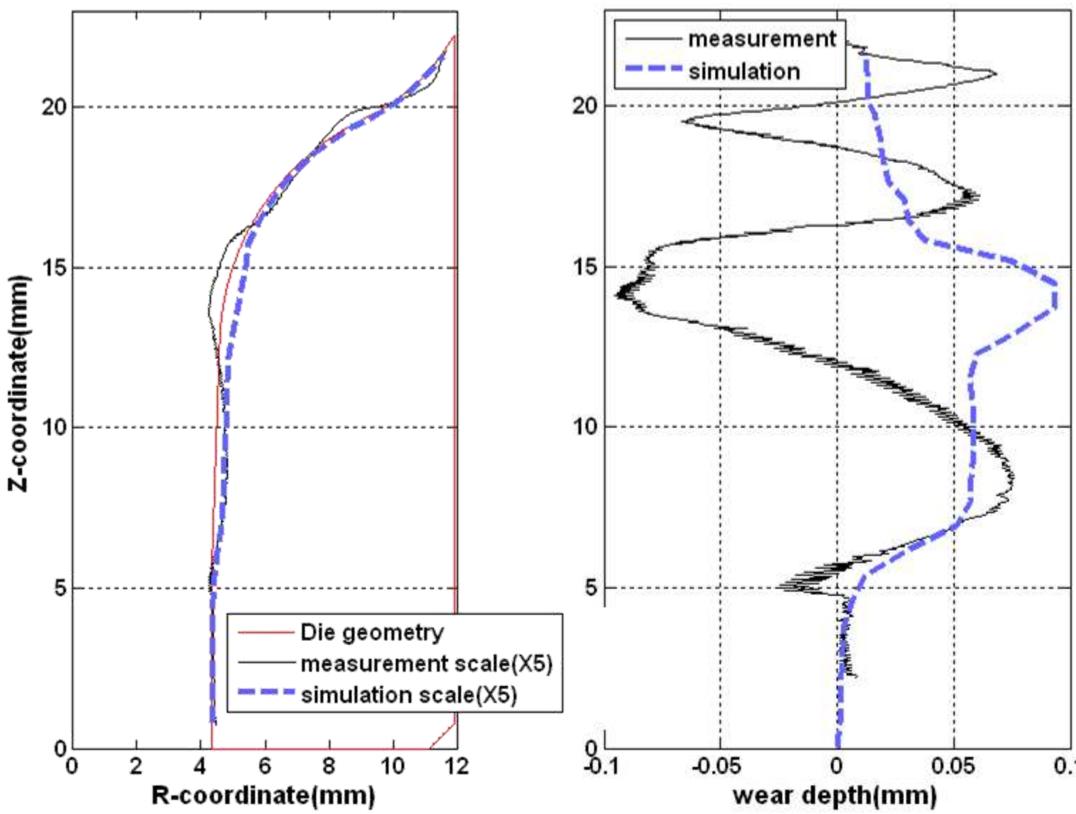

Figure 45: Predicted Wear (Combined Simulation and Wear Equation Results) ('simulation') versus CMM Measured Wear (Compensating for the Plastic Deformation) ('measurement') for Extrusion Die

There was not a second die available to compare predicted values to measured values. The first prediction did not match the experimental die profile. This is assumed to be due to phenomena that occur in the process, which cannot (at this time) be captured by FEA. Extrusion is a process with very high temperatures, high pressures, and high velocities along the die surface. This may cause microstructural changes in the die, which is hard to interpret and predict. It may also cause some sort of buckling or plastic deformation in the die, which FEM is currently unable to predict.

Results for the coining die, though not presented here, proved to be more successful than the extrusion die predictions. However, the coining die experienced far lower temperatures and velocities than the extrusion die and therefore did not have the same extreme conditions, as well.

Chapter 6: Die Cost Estimation

Die Manufacturing

Dies and molds are an important part of the manufacture of discrete parts. They are implemented in stamping, die casting, injection molding, and forging processes, to form the required parts in nearly all mass production manufacturing. Though the dies/molds for each process are all different in design and complexity, there are similarities in the manufacture of these dies. [Altan et. al., 2001]

The production differences are as follows [Altan et. al., 1999]:

- Forging/ Die Casting/ Injection Molding- Hardened tool steels (sometimes aluminum for production of plastics) are rough and finish machined from solid blocks
- Stamping- Cast to near-final geometry with a machining allowance, and then finish machined

All the processes require hard dies (> 30 HRC) and require a good surface finish with strict dimensional tolerances. These dies must have complex sculptured surfaces, which are used to form complex discrete parts. Dies and molds, similar to machine tools, may represent a small investment compared to overall value of an entire production program. However, they are crucial in determining lead times, quality, and costs of discrete parts. The quality of the dies and molds directly affect the quality of the produced parts.

Examples include molds used for injection molding lenses, dies in precision forging of automotive drive train components. [Altan et. al., 2001]

There are two main methods of die/mold production. There is the traditional method which is still in use, but is not as prevalent, and the current method of production, which has been around for the last 15 years (since the advent of High Speed Machining (HSM) and Hard Machining). The two methods are outlined below (modified from [Ahmentoglu et. al., 1997]):

Traditional Method:

1. Part Geometry Received (CAD file, Part drawing, CMM data)
2. Die Design (from standards and checked with FEM)
3. CNC rough machined from soft or hardened block (or Casting for Stamping)
4. CNC Electrode for EDM (Electrode Discharge Machining)
5. Heat Treatment of Die (if necessary)
6. EDM Hardened Die
7. Polish Die to final surface roughness
8. Check Die Dimensions with CMM (Coordinate Measuring Machine)
9. Die Tryouts

Current Method:

1. Part Geometry Received (CAD file, Part drawing, CMM data)
2. Die Design (from standards and checked with FEM)
3. CNC rough machined from hardened block (or Casting for Stamping)

4. Heat Treatment of Die (if necessary)
5. CNC finish machine die to final surface roughness (with HSM)
6. Check Die Dimensions with CMM (Coordinate Measuring Machine)

Die Tryouts

In the Current Method, it can be seen that the CNC of the EDM electrode, the EDMing of the die, and the polishing have been replaced by HSM. It is also seen that the tool steel is initially hardened and the rough and finished machined in this hardened state. This allows for significant improvements in production time and costs. [Ahmentoglu et. al., 1997]

CNC Machines and Milling of Sculptured Surfaces

CNC (Computer Numerical Controlled) milling machines are milling centers which have advanced computer controls to move the workpiece in the x-, y-, and z-axes (as well as up to 2 axes of rotation). Servo motors control each axis that the machine can move. The motors control the speed and position of each axis. These servo motors are controlled, through the computer, with G- and M- codes, which are created with CAM (Computer Aided Machining) software from a CAD model. [Arnone, 1998]

For HSM of hardened tool steels for die applications, the CNC machine must have the following specifications [Ahmentoglu et. al., 1997] [Altan et. al., 2001] [Arnone, 1998]:

- Spindle RPM- 10,000 to 50,000 depending on the tool diameter

- Feed Rates- 15 m/min or higher, when appropriate pressurized air or coolant mist is provided
- Surface Cutting Speeds- 300 to 1000 m/min depending upon the hardness of the die/mold steel and chip load
- High acceleration and deceleration capabilities of the machine tool in the range of 0.8 to 1.2 m/s^2
- High stiffness and rigidity, as well as high dynamic accuracy
- Well damped frame for absorbing of vibrations
- Tool path optimization and feed rate modifications
- Large data storage capability and high speed control and data transfer

These machines are used to create the sculptured surfaces needed for the dies/molds. These surfaces are machined using ball endmills (flat endmills can only used in 5-axis machines for sculptured surfaces) [Scurlock et. al., 1996]. Tool paths are created in CAM software based on the geometry specified by a CAD model. There are many tool path strategies that can be implemented, based on part shape and cutting time. For more information on tool paths, see [Arnone, 1998] and [Altan et. al., 2001].

Rough/Finish Milling and Surface Finish

As discussed before, the dies are first rough machined to remove most of the material and then finish machined to obtain the desired dimensions and surface finish. Roughing is performed with large heavy cuts at lower speeds. The goal is to leave a minimum amount of material for finishing. However, using relatively smaller cutters in conjunction with increased feed rates (during HSM), will increase roughing time but finishing time will be decreased, so that total milling time is reduced. Rough machining of hardened blocks will also increase machining time over roughing in soft state, but new tool set-up is eliminated for finishing. [Altan et. al., 2001] An example of time savings in machining a forging die is shown in Figure 46.

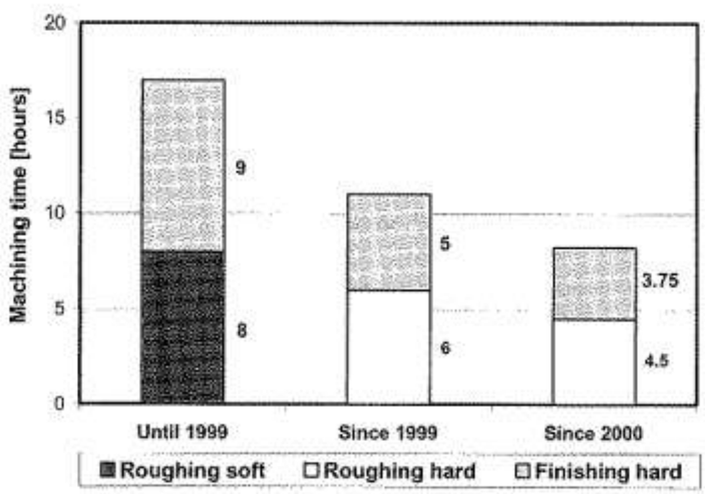

Figure 46: Reduction in Machining Time for one Forging Die [Altan et. al., 2001]

In finishing, light cuts are taken at very high speeds. This is to remove the material left by roughing and obtain the final dimensions.

To obtain the required surface finish, from finish machining to eliminate polishing, the number of finishing paths must be increased. The maximum cutter diameter is limited by the smallest die radii, therefore the only way to minimize surface finish is to decrease the width of cut (step over distance). Since cutting time is increased due to more cutter paths, the feed rates must be increased along with spindle speed to ensure net increase in cutting time. [Scurlock et. al., 1996]

Figure 47 shows a schematic of step over for a ball endmill. Where $\mathbf{a_e}$ is the step over distance, $\mathbf{a_p}$ is the depth of cut, $\mathbf{d}$ is the cutter diameter, and $\mathbf{d_w}$ is the effective cutter diameter (diameter engaged with the part).

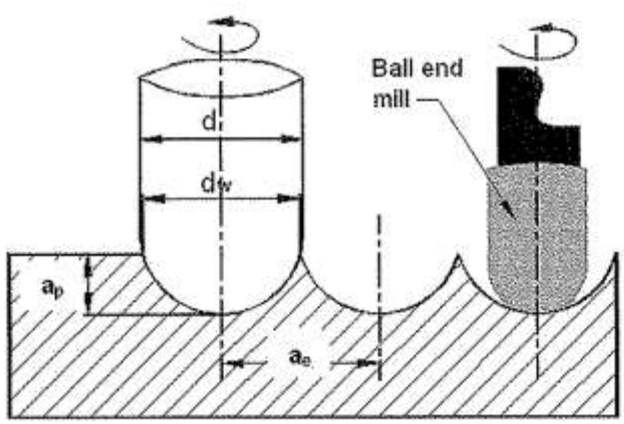

Figure 47: Ball Endmill Step Over [Altan et. al., 2001]

Optimization of the Milling Process

Most CAM software generate tool paths based on geometrical considerations. However, with other programs for tool path verification can simulate the material removal process and detect potential errors and tool collisions. [Ahmetoglu et. al., 1997]

With tool path optimization software, the spindle speed and feed rate can be regulated according to local tool engagement conditions [Ahmetoglu et. al., 1997]. This is to try to maintain a constant cutting speed and chip thickness. Tool path optimization can decrease cutting time (by 20-50%) and improve tool life, under certain conditions, compared to conventional milling. [Altan et. al., 1999]

Figure 48 shows tool path optimization to maintain constant chip thickness through a corner. Figure 49 shows feed rate modification to maintain tool load in and out of corners.

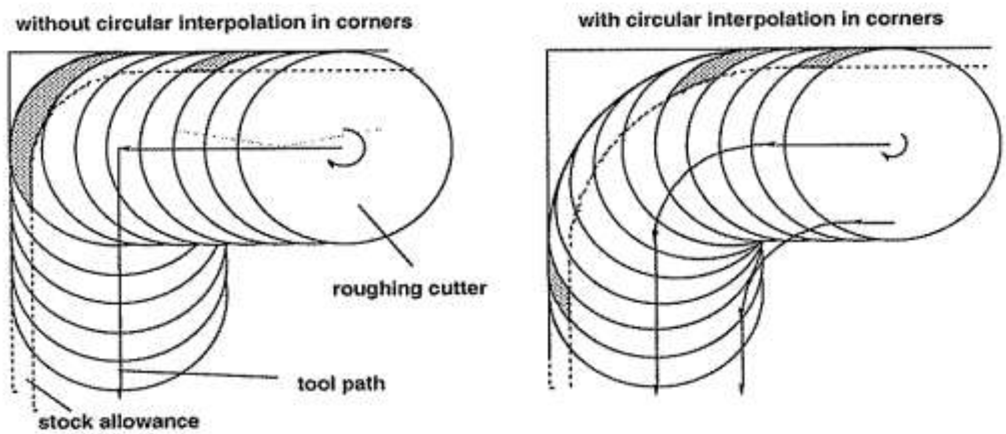

Figure 48: Tool Path Optimization [Altan et. al., 1999]

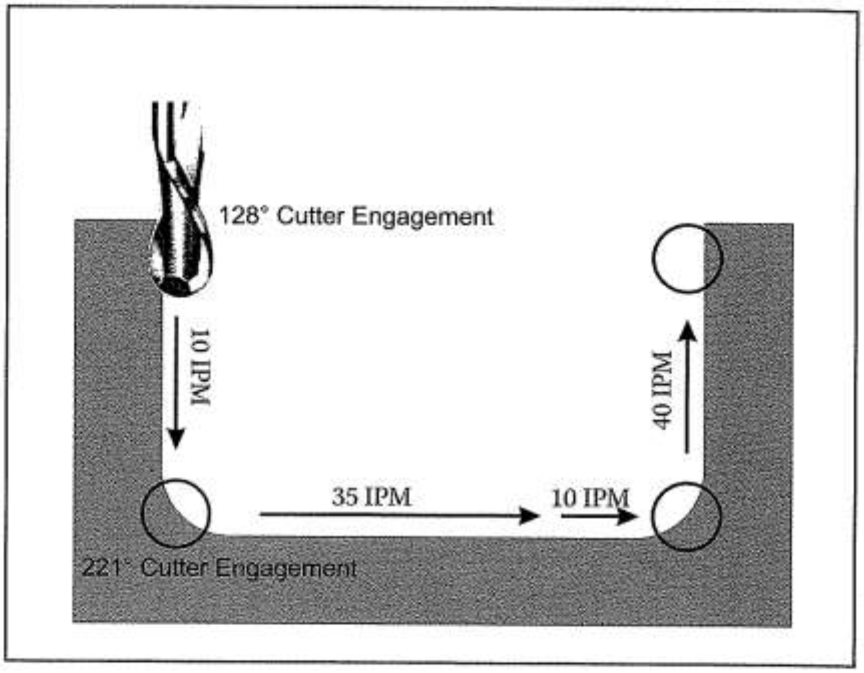

Figure 49: Feed Rate Modification [Arnone, 1998]

Estimating Time and Cost

CAM software calculates machining time by dividing the tool path length by the specified feed rate. However, this estimate will be low due to the feed rate variation during acceleration and deceleration of the tool in corners. Using a tool path optimization software (such as OPTIMILL), the actual cutting time can be estimated based on the variable feed rate. [Altan et. al., 2001]

Die/mold costs are an important factor in subsequent part costs. Total cost of the die is the combination of the material costs and the manufacturing costs of the die. The manufacturing costs are estimated by determining the time to manufacture and multiplying by hourly rates. [Boothroyd et. al., 2002]

Die design costs must be estimated, based on size and experience (assumed to already be completed). Once the die is designed, the dimensions are known and the die block size will determine the material costs. The die block is received in a hardened state, eliminating the heat treatment cost (assuming that no additional heat treatment is necessary). Thus, the material costs can be estimated.

Again assuming the die is already designed, the manufacturing costs are estimated. This is outlined by [Boothroyd et. al, 2002] for a forging die, who gives empirical formulas and charts to calculate the times (and thus the cost) to manufacture a die based on the cavity shape/size.

[Papoy et. al., 2000] provides a formula to calculate the machining cost for a stamping die. The equation is based on the die cavity surface area that is required to be machined.

Knight's Cost Model

Knight developed a cost model to estimate die costs for hammer forging and this is given by [Boothroyd et. al., 2002], discussed previously. This model is the most in depth model provided in literature and therefore the focus of this research. Hammer forgings are also the most appropriate for low quantity production runs [Boothroyd et. al., 2002]. This model can also be modified for press forging, if applicable.

The model consists of 76 variables to calculate the die cost. Of these variables, ten variables (Table 6) must be provided by the user along with three qualitative part complexity questions (i.e. Is the main axis of the part straight?; Is the die parting line flat?; and Are there any side depressions?). Eight of the ten variables are provided by the part CAD model (or drawings, if that is what is provided), as well as the three complexity questions. The last two variables are the cost of the tool steel per unit weight and the die manufacturing cost per hour.

Variable	**Units**
Part Volume, V	[cm^3]
Area of Holes, A_H	[cm^2]
Maximum Part Thickness, T	[mm]
Maximum Part Length, L	[mm]
Maximum Part Width, W	[mm]
Number of Surface Patches, N_S	[-]
Part Perimeter, P_r	[cm]
Projected Part Area, A_P	[cm^2]
Cost of Tool Steel per Unit Weight, C_t	[$/kg]
Die Manufacturing Cost per Hour, C_{man}	[$/hr]

Table 6: Input Variables for Knight's Forging Die Cost Model

The units used by the cost model are metric (kg, cm, and mm) and due to coefficients and exponents used in equations; it is not possible to change the cost model for British units without a major time investment. The simplest way to incorporate British units would be to have an initial conversion to metric units and after calculating the cost, convert back.

The part volume, length, width, and thickness are all fairly straight forward. The length is the maximum part length, width is the maximum part width, and thickness is the maximum part thickness. With the maximum part length, width, and thickness, an enveloping block can be imagined around the part, such that no portion of the part is outside of that envelope.

The perimeter and plan area are straight forward as well. They are obtained from the part in the same plane in which the die parting line will be.

The area of the holes is obtained from the holes in the part. The holes during forging will be filled and have a web in them. Therefore, the material and web thickness that occupy the holes must be included in calculations.

The number of surface patches is more difficult to determine. The number of surface patches that make up the shape in the die cavities are counted. This is an indicator of shape complexity through more complex shape features that may be present. Standard shapes (planes, cylinders, cones, etc.) are counted as one. However, sculptured features are counted as four standard shapes [Boothroyd et. al., 2002]. For more information on surface patches consult [Boothroyd et. al., 2002].

Based on the input dimensions and qualitative part shape questions, the forgings are broken into four categories (or "classes"). These classes determine which figures and tables to use when determining the forging sequence, and thus the die block size (assuming all forging operations are in one die block). For die blocks with only one cavity, the class would determine how many die blocks were needed.

The die block size is determined by the input dimensions as well as the number of operations in the forging sequence. Die block volume allows for the material costs of the die to be calculated (based on the price per kilogram of tool steel).

The die block manufacturing cost (cost to machine the die cavity) is slightly more difficult to determine. The cost is determined by estimating the time to produce the die cavity. Based on a modification of guidelines presented by the FIA (Forging Industry Association), Knight set up a series of empirical formulas to account for each step of the die making process.

The procedure to estimate die manufacturing time includes formulas for:

i. Block Preparation Time
ii. Layout Time
iii. Milling Time
iv. Bench Work Time
v. Planing Time
vi. Flash Gutter Machining Time
vii. Edger Die Manufacturing Time (If an edger die is required)

viii. Finishing/Polishing Time

The cost to manufacture is then estimated by summing the times calculated, for each step listed, and multiplying by the cost per hour to manufacture the die (provided by the user). Now that both costs (die material and die manufacturing costs) are estimated, the total die cost is determined by adding the two costs together.

This procedure is relatively simple and easy to implement if the final part drawings or CAD model can be provided. The cost model developed by Knight was written into an Excel file as a code. The file will calculate the die costs based on the ten input variables and three questions' answers provided by the user.

Validation

Based on forging die data obtained from Weber Metals, Knight's model was tested. The data was for around 40 aluminum forgings, which varied in size from 60 to 8000 in^3. The forgings were mostly aerospace parts used in a wide range of applications. The data collected from the forgings were obtained from CAD files and included the volume and surface area of the finished part, as well as the volume, surface area, length, width, and thickness of the enveloping box. Cost of the die material and manufacturing costs were collected. The data collected for the finished part was also collected for any blocker dies, which may have been needed.

The number surface patches was found difficult to determine, because the guidelines for determining patches was somewhat vague. The plan area and part perimeter were also required to be determined. Upon testing 10 forging samples, Knight's model was determined to be inadequate to estimate the die block size (which determines the cost), as well as the total manufacturing cost. Therefore, it was deemed necessary to develop a new cost model, which would be a modification of Knight's model that seemed to have a good methodology.

New Cost Model

The new model would be based on Knight's cost model and the data obtained from Weber Metals. Since Weber produces low quantity productions, this was a reasonable data source for the new model. However, the size of the forgings, and hence the forging die, were larger than conventional parts, requiring some modification of the data to be more suitable to the desired goal. These changes were based on recommendations by Weber, which used larger die blocks than necessary to allow for resinking and prevention of die failure. Therefore, the die blocks and die material costs are larger than what would be required and this was compensated by taking 80% of the die costs.

Methodology

Material Costs

The die block dimensions were determined with a simple estimation based on the envelope dimensions (length, width, and thickness) (Figure 50). The block length is equal to 1.0 times the depth of the die cavity added to each end, which means 2.0 times the cavity depth plus the part length (Equation 12). The block width uses the same procedure as the length and adds 2.0 times the cavity depth to the width (Equation 13). The cavity depth is assumed as one-half of the maximum part thickness (envelope thickness).

$$L' = L + 2D \qquad \text{Equation 12}$$

$$W' = W + 2D \qquad \text{Equation 13}$$

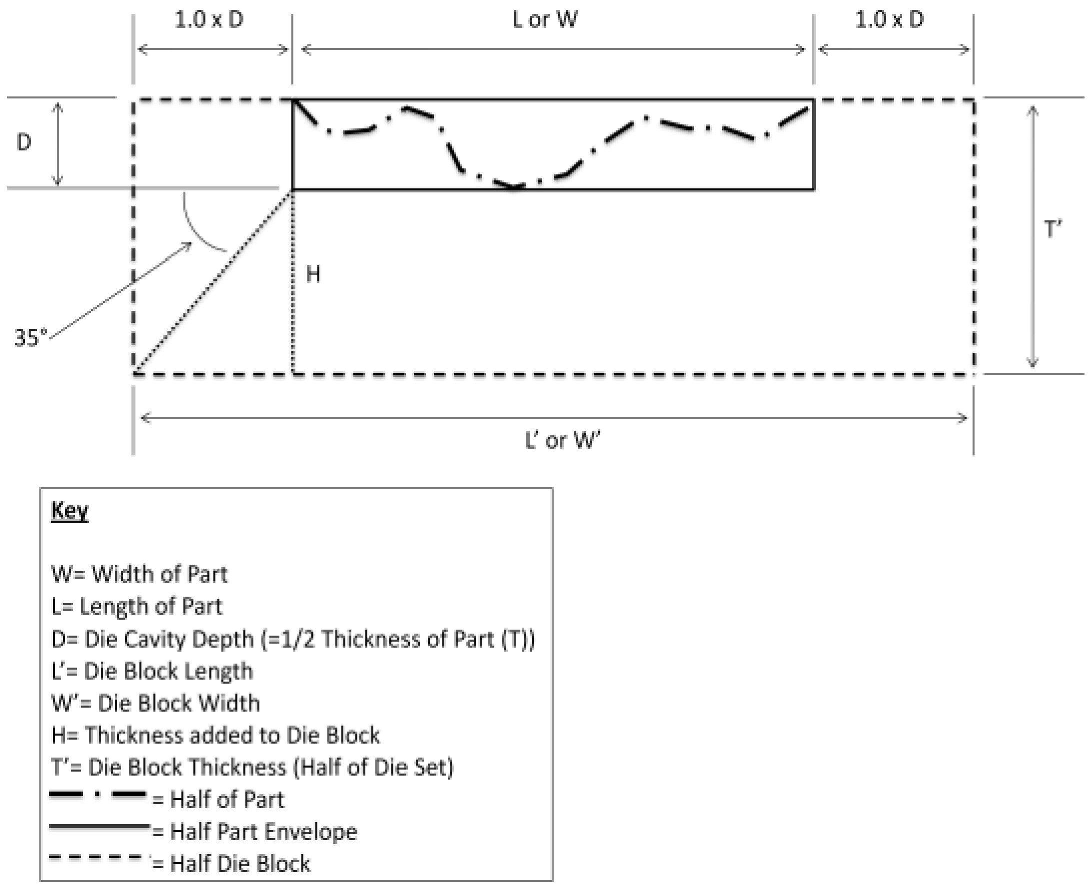

Figure 50: Schematic of Die Block Size Estimation

To obtain the die block thickness, a 35° (to the bottom of the envelope, i.e. horizontal) line is drawn from the edge of the envelope to the vertical from the end of the block length (determined above). The equation for the block thickness is given in Equation 14.

$$T' = D + H = (1.0\tan(35°) + 1)D = \frac{(1.0\tan(35°) + 1)}{2}T \qquad \text{Equation 14}$$

The material cost is then the volume of the die block (length x width x thickness) times the density times the number of die sets times 2 (for two halves for each set) (Equation 15).

$$Cost(C_{mat}) = L'*W'*T'*\rho*\frac{Cost}{weight}*DieSets*2Halves \qquad \text{Equation 15}$$

Where Density (ρ)=0.289 lbs/in^3 and Cost/weight= about \$1.60/lb for tool steel. Die Sets is dependent on the part difficulty (more difficult = more die sets) and 2 is constant because there will always be two halves to a die set.

Shape Classification and Forging Complexity (Future Work)

From the Weber data, it is necessary to develop a shape classification system, as well as a forging complexity variable. The classification system will help separate the forgings into classes, which can be used to determine difficulty of the part and how many operations required to forge the part (i.e. one or two blocker dies). The complexity factor will be used to give a numerical value, for which the cost calculations can be multiplied by to give a higher cost for more difficult parts.

The classification system should be around six to eight categories, which will give somewhat specific results without being too general or complex. The system should be similar to Knight's system, which separated forgings based on the thickness versus length and width versus length of the envelope. It also allowed for sub-categories based on whether the part had side depressions or the dies required a skewed parting line, both of which increase forging difficulty.

The forging (or shape) complexity factor should allow for increased cost for increased difficulty. The ways to determine this factor are numerous. One can use: the surface area versus the volume of the part, plan area and part perimeter, cross-sectional area of the part versus cross-section of a circle or rectangle of the same area, volume of an envelope versus the part volume (as Knight's model), as well as many others.

For future work, the classification and complexity systems will be difficult to determine, but are probably the most important factors in producing a good estimate of costs.

Manufacturing Costs (Future Work)

The manufacturing costs are also difficult to estimate. To have empirical formulas which account for all forging possibilities is impossible. However, the easiest way to estimate cost is with a regression analysis of cost and part dimensional data. If it can be proven, through the Weber data, that the geometry is related to the manufacturing cost, then the estimation can be based on a small amount of dimensional data (which may be all that is known in the early stages of quoting).

Validation

Only the material cost model has been started at this time and it looks to be fairly accurate. However, the cost model (material and manufacturing), as well as the shape classification system and complexity factor, need to be refined and developed further in the future.

Chapter 7: Summary and Conclusions

Die Wear

The two case studies presented showed a very useful way in which FEM can be applied. Both studies were of the die wear that occurs in elevated temperature extrusion of strong steel alloys. This extrusion causes high velocities and pressures, which are in addition to the already high working temperatures. The combined effect is accelerated abrasive die wear due to thermal softening and rubbing between the workpiece and die.

However, abrasive wear is not the only form of die failure acting upon the die at elevated temperatures. Plastic deformation is also occurring due to high temperatures and pressures during extrusion. Therefore, it is impractical to predict wear without first predicting and accounting for the plastic deformation.

FEM is used to obtain the process variables (temperatures, pressures, velocities, etc.) to predict wear, as well as the stresses and deformations of the dies to predict the plastic deformation. FEM is even used to determine the flow stress of the die tool steel (which is not usually available in literature) using a limited amount of data, such as the ultimate tensile strength, yield strength, and hardness as functions of temperature (which is provided by the manufacturer).

After the wear and plastic deformation are estimated, FEM can then be used to optimize the forming process. Whether it be through changes in material (workpiece or die), press speed, operating temperature (of the workpiece or die), or die shape, FEM can be used effectively to improve the forming process.

However, the FEM is limited in its ability to account for all the variables in extreme conditions (very high temperatures, high pressures, and high velocities on the die surface) during valve extrusion. Therefore, the experimental and predicted die surface profiles were different and the explanation is unknown. Possible microstructural effects of the conditions in valve extrusion may be the cause, as well as some sort of internal buckling or plastic deformation of the die, which are not captured by current FEA predictions.

Die Cost

Die cost is an important and critical portion of the forging process cost. It is often difficult to predict the die cost, especially in the early stages of quoting when a limited amount of information is known. Therefore, it is advantageous to determine a relationship between the part geometry and die cost, because the final part geometry is known early in the process.

There is also limited information about die cost estimation in the literature. This seems to be seen as a proprietary procedure at companies and therefore nothing is published about it. Each company does costing a slightly different way and usually it is based on experience and not necessarily a scientific procedure.

More study needs to be performed, in this field, in order to determine the geometrical relationships to die cost. If such a relationship is found, not only can forgers be helped, but also the people trying to buy forgings. They may or may not have experience in forging and therefore could benefit from an empirical way to determine die cost. With a decent estimate of die cost, then the purchaser would have an idea of what the cost is before quotes are obtained. Then company quotes can be compared with the estimate previously obtained and this allows for a more informed decision.

List of References

[Ahmetoglu et. al., 1997]	Ahmetoglu, M., Akherman, N., and Altan, T., "Systems Approach is Key to Die Moldmaking", Tooling & Production, May 1997, pg. 39
[Akgerman et. al., 1999]	Akgerman, N. & Altan, T., "Common Sense in High Speed Milling of Dies and Molds", Mold Making Technology Journal, Oct. 99, p.29
[Altan et. al., 2005]	Altan, T., Ngaile, G. and Shen, G. "Cold and Hot Forging: Fundamentals and Applications", ASM International, 2005.
[Altan et. al., 2001]	Altan T. and Lilly B., "Manufacturing of Dies and Molds", Key Note Paper, CIRP, 2001, Annnals of CIRP, v.2, p.405
[Altan et. al., 1999]	Altan, T. et al. "High Performance Machining for Die/ Mold Manufacturing- R & D in Progress", from "Machining Impossible Shapes", by G.J. Olling, ISBN- 412-84680-2, p.293
[Archard, 1953]	Archard, J., "Contact and Rubbing of Flat Surfaces", Journal of Applied Physics, Vol. 24, 1953, pp. 981-988.
[Arnone, 1998]	Arnone, M., High Performance Machining, Hanser Gardner Publications, 1998 ISBN- 1-56990-246-1
[ASM, 2005]	ASM Handbook, Volume 14A- Metalworking: Bulk Forming, ASM International, 2005, ISBN 0-87170-708-X
[Babu, 2004]	Babu, S., "A Material Based Approach to Creating Wear Resistant Surfaces for Hot Forging", PhD Dissertation, The Ohio State University, 2004.
[Behrens et. al., 2005]	Behrens, B.A., and Schaefer, F., "Prediction of Wear in Hot Forging Tools by Means of Finite Element Analysis", Journal of Materials Processing Technology, Vol. 167, 2005, pp. 309-315.

[Behrens, 2008] Behrens, B.A., “Finite Element Analysis of Die Wear in Hot Forging Processes”, CIRP Annals- Manufacturing Technology, Vol. 57, 2008, pp. 305-308.

[Berg et. al., 1996] Berg, T., Rodriguez, C., et al (including Altan), “Tool Path Optimization for Finish Milling of Die and Mold Surfaces - Software Development”, Transactions of NAMRC XXIV, May 1996, SME, pp. 81-86

[Bohler, 2009] “Bohler W320- Hot Work Tool Steel”, W320 data sheet, Bohler website, 2009, www.bohler-edelstahl.com/english/3383_ENG_HTML.php, March 2010

[Boothroyd et. al., 2002] Boothroyd, G., Dewhurst, P., and Knight, W., Product Design for Manufacture and Assembly, Second Edition, Marcel Dekker, 2002, ISBN 0-8247-0584-X

[Burte et. al., 1989] Burte, P., Semiatin, S., and Altan. T., “Measurement and Analysis of Heat Transfer and Friction During Hot Forging (Final Report)”, ERC for Net Shape Manufacturing, Report No. 89-20-B, 1995, The Ohio State University.

[Collins, 1981] Collins, J. A., Failure of Materials in Mechanical Design, John Wiley and Sons., 1981.

[Dahl et. al., 1998] Dahl, C., Vazquez, and V., Altan, T., “Effect of Process Parameters on Die Life and Die Failure in precision Forging”, ERC for Net Shape Manufacturing, Report No. NSM-98-R-015, 1998, The Ohio State University.

[Dahl et. al., 1999a] Dahl, C., Vasquez, V., and Altan, T., “Final Report on the Effect of Process Parameters on Die Failure and Die Life in Precision Forging”, ERC for Net Shape Manufacturing, Report No. 99-R-14, 1998, The Ohio State University.

[Dahl et. al., 1999b] Dahl, C., Vasquez, V., and Altan, T., “Analysis and Prediction of Die Wear in Precision Forging Operations”, ERC for Net Shape Manufacturing, Report No. 99-R-21, 1999, The Ohio State University.

[Deshpande et. al., 2009] Deshpande, M., Choi, C., Groseclose, A., and Altan, T., "Estimation of Die Wear in Forging of Engine Valves: Progress Report II", ERC for Net Shape Manufacturing, Report No. ERC/NSM-09-R-11-II, 2009, The Ohio State University.

[Doege et. al., 1994] Doege, E., Naegele, H., and Schliephake, U., "Aspects of Wear Prediction in Precision Forging", Proceedings of the Institution of Mechanical Engineers, Vol. 280, 1993, pp. 111-119.

[Doege et. al., 2001] Doege, E., Huskic, A., Barnert, L., Gulde, M., and Hornhardt, Ch., "Reduction of Wear of Forging Dies by Use of New Technologies", New Developments in Forging Technology, University of Stuttgart, 2001, pp. 315-327.

[Fallböhmer et. al., 1998] Fallböhmer, and Altan, T., "The Application of PCBN Cutting Tools in Die and Mold Manufacturing", Ohio State University ERC/NSM, Report No. ERC/NSM-98-R-8-D, 1998

[Fallböhmer et. al., 1995] Fallböhmer, Tönshoff, and Altan, T., "High Speed Milling of Dies and Molds-State of the Art Report", Ohio State University ERC/NSM, Report No. ERC/NSM- 95-17-D, 1995

[Field, 2002] Field, R., "High Speed Machining of Dies and Molds (Revisited)", *Millstar Tech Articles*, 2002, www.millstar.com/ms_tech001, February 2010

[Groseclose et. al., 2008] Groseclose, A., Choi, C., Gonzalez-Mendez, J., and Altan, T., "Estimation of Die Stresses and Wear in Warm Forging of Steel Pinion Shafts", ERC for Net Shape Manufacturing, Report No. ERC/NSM-08-R-34, The Ohio State University.

[Holm, 1946] Holm, R., "Electrical Contacts", Almquist and Wiksells, Stockholm, Section 40, 1946.

[Hollomon et. al., 1945] Hollomon, J.H., and Jaffe, L.D., Time-Temperature Relations in Tempering Steel, Trans. AIME, Vol 162, 1945, p 223-249.

[Kang et. al., 1999a] Kang, J., Park, I., Jae, J., and Kang, S., “A Study on a Die Wear Model Considering Thermal Softening: (I) Construction of the Wear Model”, Journal of Materials Processing Technology, Vol. 96, 1999, pp. 53-58.

[Kang et. al., 1999b] Kang, J., Park, I., Jae, J., and Kang, S., “A Study on a Die Wear Model Considering Thermal Softening: (II) Application of the Suggested Wear Model”, Journal of Materials Processing Technology, Vol. 94, 1999, pp. 183-188.

[Kim et. al. 2005] D. H. Kim, H. C. Lee, B. M. Kim, K. H. Kim, “Estimation of die service life against plastic deformation and wear during hot forging processes”, Journal of Materials Processing Technology, Vol.166, pp.372-380, 2005

[Klein et. al., 1990] Klein, Lilly, Kropp, and Altan, T., “Development of Rough Milling Strategies for Efficient Production of Die and Molds”, Ohio State University ERC/NSM, Report No. ERC/NSM- 90-37-D, 1990

[Nachi-Fujikoshi, 2008] “DURO for hot work”, DURO-F1 data sheet, Nachi-Fujikoshi website, 2008, www.nachi-fujikoshi.co.jp/eng/web/pdf/S4302E.pdf, March 2010

[Painter et. al., 1996] Painter, B., Shivpuri, R., and Altan, T., “Prediction of Die Wear During Hot-Extrusion of Engine Valves”, Journal of Material Processing Technology Vol 59, 1996, pp. 132-143.

[Painter et. al., 1995] Painter, B., Shivpuri, R., and Altan, T., “Computer-Aided Techniques for the Prediction of Die Wear During Hot Forging of Automotive Exhaust Valves”, ERC for Net Shape Manufacturing, Report No. B-95-06, 1995, The Ohio State University.

[Papoy et. al., 2000] Papoy, M. and Altan, T. “The Implementation and Impact of High Performance Machining in Die Casting Operations – Bringing the Science into Service,” NADCA Conference, Chicago, Nov. 6, 2000.

[Scurlock et. al., 1996] Scurlock, R. and Fallböhmer, P., "Milling Sculptured Surfaces", Cutting Tool Engineering Magazine, September 1996, p. 35

[Shaw, 1989] Shaw, M., "Metal Cutting Principles", Oxford, Oxford Science Publications, 1989.

[Sheljaskow, 2001] Sheljaskow, S., "Tool Lubricating Systems in Warm Forging", Journal of Materials Processing Technology, Vol. 113, 2001, pp. 16-21.

[Shirgaokar, 2008] Shirgaokar, M., "Technology to Improve Competitiveness in Warm and Hot Forging: Increasing Die Life and Material Utilization", PhD Dissertation, The Ohio State University, 2008.

[Siegert et. al., 1997] Siegert, K., and Altan T., and Nakagawa T., "Development and Manufacture of Dies for Car Body Production", Annals of CIRP, vol. 46/2/1997, pg. 535

[Tulsyan, 1993] Tulsyan, R., Shivpuri, R., and Altan, T., "Investigation of Die Wear in Extrusion and Forging of Exhaust Valves", ERC for Net Shape Manufacturing, Report No. B-93-28, 1993, The Ohio State University.

[Wertheim et. al., 2002a] Wertheim, R., Harpaz, J., and Satran, A., "New Tool Concepts for Machining Dies and Molds" Part 1, *Mold Making Technology*, 2002, www.moldmakingtechnology.com/articles/040202, February 2010

[Wertheim et. al., 2002b] Wertheim, R., Harpaz, J., and Satran, A., "New Tool Concepts for Machining Dies and Molds" Part 2, *Mold Making Technology*, 2002, www.moldmakingtechnology.com/articles/050202, February 2010

[Yazar et. al., 1994] Yazar, Z., Koch, K-F, Merrick, T. and Altan, T. "Feed Rate Optimization Based on Cutting Force Calculations in 3-Axis Milling of Dies and Molds with Sculptured Surfaces", International Journal for Machine Tools and Manufacture, V.34, No. 3, pp. 365-377, 1994